# Mixing in two-dimensional shear flow with smooth fluctuations

Nikolay A. Ivchenko ,[*] Vladimir V. Lebedev,[†] and Sergey S. Vergeles [‡]
*Landau Institute for Theoretical Physics, Russian Academy of Sciences, 1-A Akademika Semenova av., 142432 Chernogolovka, Russia*
*and National Research University Higher School of Economics, Faculty of Physics, Myasnitskaya 20, 101000 Moscow, Russia*

(Received 25 September 2023; accepted 22 May 2024; published 15 July 2024)

Chaotic variations in flow speed up mixing of scalar fields via intensified stirring. This paper addresses the statistical properties of a passive scalar field mixing in a regular shear flow with random fluctuations against its background. We consider two-dimensional flow with shear component dominating over smooth fluctuations. Such flow is supposed to model passive scalar mixing, e.g., inside a large-scale coherent vortex forming in two-dimensional turbulence or in elastic turbulence in a microchannel. We examine both the decaying case and the case of the continuous forcing of the scalar variances. In both cases dynamics possesses strong intermittency, which can be characterized via the single-point moments and correlation functions calculated in our work. We present general qualitative properties of pair correlation function as well as certain quantitative results obtained in the framework of the model with fluctuations that are short correlated in time.

DOI: 10.1103/PhysRevE.110.015102

## I. INTRODUCTION

Mixing is a process of homogenization of a scalar field in fluids, such as temperature or a concentration of impurities, accelerated by means of advection. The acceleration is especially effective in chaotic flows which are characterized by irregular fluctuations of the flow velocity in space and/or time. This random part speeds up stirring process for the scalar, which causes stretching of its blobs into lamellae with their subsequent folding. The thinning of lamella in its transverse direction initiates the molecular diffusion that finalizes the mixing. The mixing process has nontrivial statistical properties (see, e.g., [1,2]), and a problem of passive scalar considers the limit when the field's back reaction to the flow is negligible.

After ascertainment of the statistical properties of developed isotropic three-dimensional [3] and two-dimensional [4] turbulence, the theory of mixing in a statistically isotropic flow within inertial interval [5,6] and at scales below the Kolmogorov (viscous) one [7] became its natural development; see also reviews [8,9]. The isotropic turbulence is an idealized model of the small-scale pulsations imposing on time-averaged large-scale flow component. However, the gradient of the mean flow entails anisotropy that varies statistical properties of both the pulsations and the mixing process.

The degree of the variation depends on the ratio of gradients magnitudes in the mean flow to those in the turbulent part. In case of the near-wall turbulence [10,11] in three-dimensional flow they are of same order. Along with the Kolmogorov scaling for velocity lasting at the small scales within inertial range [12], anisotropy of flow spreads down there as well. It produces so-called ramp-cliff structures [9] and anisotropy in the scalar gradient [13] in the case of Schmidt number $\mathrm{Sc} = \nu/\kappa \sim 1$, where $\nu$ is the kinematic viscosity of the fluid and $\kappa$ is the diffusion coefficient of the scalar. Another case, the limit where mean flow is prevailing over turbulent pulsations, takes place under some conditions. Axisymmetric vortical flow and near-wall flow are the simplest forms in a geometrical sense. In both velocity gradient around a Lagrangian trajectory established by the mean flow remains unchanged thus forming a shear flow. An example of the first type is large-scale coherent vortex emerging in two-dimensional turbulence due to the inverse energy cascade [14–17] that motivated the current study. An elastic turbulent flow of a polymer solution in a microchannel [18] is of the second type. For all of them velocity energy spectra are steep enough [19–21], so one can assume the fluctuations on the background of the shear flow are large scale as well and thus are smooth. Suppression of small-scale turbulent pulsations means that the effective Schmidt number Sc is increased. Indeed, the Kolomogorov scale should be replaced by the flow scale $R$, so the Schmidt number $\mathrm{Sc} \sim R^2/r_\kappa^2$ [8], where the Batchelor (diffusion) scale $r_\kappa \sim \sqrt{\kappa/\bar{\lambda}}$ and $\bar{\lambda}$ is the Lyapunov exponent of the flow. The same assumption should be applicable to describe mixing in laminar vortex flow of Newtonian fluid [22,23], where the source of the flow fluctuations are imperfect boundary conditions as well as deviations of force driving the flow.

In this work we provide an analytical study of a passive scalar field $\vartheta$ mixing in the flow with a spatially smooth divergent-free velocity field with strong static shear component and relatively weak fluctuations at large Schmidt number. We consider either the decay of the passive scalar or its continuous forcing. For the decay problem, one starts with certain initial distribution of the passive scalar and examines the evolution of its statistical characteristics. Experimentally, decay of the passive scalar was observed in channels [24],

[*]Contact author: ivchenko@itp.ac.ru
[†]Contact author: lebede@itp.ac.ru
[‡]Contact author: ssver@itp.ac.ru

 

microchannels [25], and soap films [26,27], where the passive scalar supply is organized at the input to the flow. The decay problem for a spatially smooth velocity field with isotropic statistics of turbulent fluctuations in the absence of the mean flow was treated analytically in Refs. [28,29], where moments of the passive scalar were considered. The examination was extended to high-order correlation functions in Ref. [30]. The case of scalar mixing in constant shear flow, which makes the advection deterministic, was considered in Ref. [31]. The case when a random component is imposed on the shear flow was considered numerically in Ref. [32] within the Kraichnan model. The continuous statistically homogeneous in time stochastic forcing of passive scalar leads to a statistically steady state providing statistics of the random flow is homogeneous in time as well [8,9]. In the large Schmidt number limit, passive scalar cascade develops the Batchelor spectrum in a wide range from the Kolmogorov scale down to the Batchelor scale [5–7].

The general picture of passive scalar evolution can be considered in terms of a separate blob. The molecular diffusion effects can be neglected at scales larger than the Batchelor length, where scalar mixing reduces to its advection by the flow. In a stationary shear flow, any vector $\boldsymbol{\ell}$ connecting two close Lagrangian trajectories grows linearly as time goes, aligning along the streamlines. However, random component of the flow causes the tumbling processes, when the direction of $\boldsymbol{\ell}$ is inverted [33,34], so it deviates from the streamlines at time average. As a result, the flow's random component enables the blob to stretch exponentially in time in one direction and yet to shrink in transverse direction, permanently experiencing tumblings. In experiment, tumblings can be visualized by observing the polymer elongations; see Refs. [35,36]. Such processes of passing through an unstable stationary point by virtue of fluctuations take place in various nonequilibrium physical systems [37]. The diffusion effects are switched on when the lateral size of the blob is diminished down to the Batchelor scale. Then the lateral size of the blob is stabilized at this scale, whereas the longitudinal size of the blob continues to grow exponentially. This means dissolution of the blob via mixing due to the concentration inside it is inversely proportional to the its area.

The paper is organized as follows. In Sec. II we discuss the general properties of passive scalar dynamics and study statistics of Lagrangian trajectories that describe mixing without diffusion. Some analytical results are obtained in the framework of model where the random flow is short correlated in time. After that we include diffusion effects into our consideration and examine moments and correlation functions of the passive scalar. The decay problem is analyzed in Sec. III, where the passive scalar evolution starts from initial distribution in a form of axially symmetric blobs' ensemble. The key component in the investigation of the passive scalar statistics is averaging over the flow statistics. Since the random flow is assumed to have the correlation length much larger than the sizes of the blobs, it coherently influences many blobs. This leads to strongly non-Gaussian statistical properties of the passive scalar that are studied in present work. The continuous forcing of scalar is considered in Sec. IV; it is realized via bringing new statistically independent blobs into the system by an external source in our model, and after that each evolves as in the decay case. Part of the results about the single-point moments was presented in [38]. In the present work we choose an expedient technique, which includes rescaling in the streamwise direction, that reformulates the problem and enables us to compare it directly to the isotropic turbulence case. Moreover, here we analyze spatial correlation functions dependency at different points. Some technical details are presented in Appendixes.

## II. GENERAL RELATIONS

In this section we introduce basic relations required to examine passive scalar statistics. We consider the scalar field $\vartheta(t,\boldsymbol{r})$ carried by an incompressible fluid flow while being diffused and supplied by an external source (pumping). The equation governing passive scalar dynamics is

$$\partial_t\vartheta + (\boldsymbol{v}\cdot\nabla)\vartheta = \kappa\Delta\vartheta + f, \quad \nabla\cdot\boldsymbol{v} = 0, \tag{1}$$

where $\boldsymbol{v}$ is the flow velocity, $f$ is the external source of the scalar, $\kappa$ is its molecular diffusion coefficient, and $\Delta$ designates the Laplacian. We assume that the flow velocity $\boldsymbol{v}$ has a random component that is small compared to its constant part and forcing $f$ is a stochastic quantity which has characteristic scale $L$ in space. We assume that the influence of the diffusion at scale $L$ is weaker not only than one from the constant part of the velocity, but also than the effect of stirring acceleration caused by the random part of the velocity. All the criteria are formulated below [see (8) and (45)].

For our limit of weak diffusion, it is reasonable to study first separately the evolution of the passive scalar in the absence of it. If one neglects the diffusion term in Eq. (1), then its solution can be written in terms of Lagrangian trajectories $\boldsymbol{q}(t)$ that are governed by the equation

$$\partial_t\boldsymbol{q}(t) = \boldsymbol{v}(t,\boldsymbol{q}). \tag{2}$$

The solution of the diffusionless equation (1) with the initial condition $\vartheta(0,\boldsymbol{r})$, taken at $t=0$, is

$$\vartheta(t,\boldsymbol{r}) = \vartheta[0,\boldsymbol{q}(0)] + \int_0^t dt_1\, f[t_1,\boldsymbol{q}(t_1)]. \tag{3}$$

Here $\boldsymbol{q}$ is the Lagrangian trajectory passing through the point $\boldsymbol{r}$ at the time $t$, $\boldsymbol{q}(t)=\boldsymbol{r}$.

Further in the work we examine the case where the velocity field $\boldsymbol{v}$ is smooth, i.e., it can be expanded into Taylor series with the convergence radius larger than all scales characterizing the passive scalar evolution. The scalar spatial distribution is influenced mainly by the smooth component of the flow, whereas the effect of its relatively weak small-scale fluctuations can be included into renormalization of the diffusion coefficient $\kappa$ [39].

### A. Statistics of Lagrangian trajectories

Let us examine statistical properties of the difference $\boldsymbol{\ell} = \boldsymbol{q}_1 - \boldsymbol{q}_2$ between two Lagrangian trajectories. Our interest is the probability density function (PDF) for $\boldsymbol{\ell}$ at different times assuming some fixed initial value of $\boldsymbol{\ell}$ or its initial probability distribution. For a scalar as an ensemble of blobs with homogeneous spatial statistics the PDF can be thought of as probability for both starting and ending points of $\boldsymbol{\ell}$

getting inside of it. Vectors $\boldsymbol{\ell}$ and $-\boldsymbol{\ell}$ are equivalent for the description of the scalar spatial distribution in this sense, thus $\boldsymbol{\ell}$ can be called a director. First, we formulate the dynamical equation for $\boldsymbol{\ell}$, and then extract its statistical properties by averaging over the statistics of the random flow.

Assuming that the difference $\boldsymbol{\ell}$ lies inside the region of the smoothness of the velocity field, we find from Eq. (2)

$$\partial_t \ell_i = \ell_k \partial_k v_i, \tag{4}$$

where we kept the main term of the expansion of the velocity field $\boldsymbol{v}$ in the Taylor series. The velocity gradient $\partial_k v_i$ in Eq. (4) is a function of time, determined by structure of the velocity field in the vicinity of the close Lagrangian trajectories $\boldsymbol{q}_1$ and $\boldsymbol{q}_2$. The flow incompressibility condition, $\nabla \cdot \boldsymbol{v} = 0$, leads to the property that the gradient matrix is traceless: $\partial_k v_k = 0$.

Further we focus on the two-dimensional dynamics. We examine the case where the velocity field $\boldsymbol{v}$ contains both the regular (deterministic) contribution and the fluctuating (random) one. The regular contribution is assumed to be a shear flow. We chose the axes $X, Y$ of the reference frame to fix the shear flow velocity as $v_x = \Sigma y$, where $\Sigma$ is the shear rate which is presumed to be positive for definiteness. Then we obtain from Eq. (4)

$$\partial_t \ell_x = \Sigma \ell_y + \ell_x \partial_x u_x + \ell_y \partial_y u_x, \tag{5}$$

$$\partial_t \ell_y = \ell_x \partial_x u_y + \ell_y \partial_y u_y, \tag{6}$$

where $\boldsymbol{u}$ is the fluctuating part of the velocity. Its statistical properties are assumed to be homogeneous in time and space.

The fluctuating part of the velocity $\boldsymbol{u}$ is supposed to be relatively weak. To characterize the weakness, one introduces the tensor

$$D_{ijkl} = \int_0^\infty dt\, \langle \partial_i u_j(t) \partial_k u_l(0) \rangle, \quad D_{jjkl} = D_{kljj} = 0. \tag{7}$$

All elements of the tensor $D$ are assumed to be of the same order. The angular brackets in Eq. (7) and subsequently denote averaging over statistics of the random flow $\boldsymbol{u}$. In an experiment, the averaging should be implemented over the volume where the velocity statistics is spatially homogeneous and/or over realizations in experimental runs. As is shown in Appendix B, starting from (B4), the only element of our interest is $D = D_{xyxy}$ due to the anisotropy dictated by the shear flow. The weakness of the random flow in comparison with the shear flow means

$$D \ll \Sigma. \tag{8}$$

The dynamics of the vector $\boldsymbol{\ell}$ is peculiar [33] due to fluctuations of $\ell_y$, caused by the random part of the velocity; see Eq. (6). The main term in right-hand side of Eq. (5) is $\Sigma \ell_y$. Therefore, if $\ell_y > 0$ then $\ell_x$ grows towards positive values. However, if $\ell_y$ becomes negative, $\ell_x$ starts to diminish and then changes its sign and grows towards negative values. This process when $\ell_x$ changes abruptly its sign is called tumbling. Precise streamline alignment of $\boldsymbol{\ell}$ is an unstable stationary point for the vector direction in dynamics with constant shear only. The fluctuating component of the flow enables tumbling processes by changing $\ell_y$ sign. Tumblings occur aperiodically in a characteristic time $D^{-1/3}\Sigma^{-2/3}$.

Between the tumblings $\ell_x \gg \ell_y$. The ratio $\ell_y/\ell_x$ can be estimated as $(D/\Sigma)^{1/3} \ll 1$ then, being the characteristic angle between the director and the streamlines. However, during each tumbling $\ell_x$ diminishes by a large factor. To avoid particular analysis of the tumbling processes, we exploit the following parametrization of the vector $\boldsymbol{\ell}$:

$$(D/\Sigma)^{1/3} \ell_x = l_0\, e^{\varrho} \cos\phi, \quad \ell_y = l_0\, e^{\varrho} \sin\phi, \tag{9}$$

where $l_0$ is a constant determined by the initial value of $\boldsymbol{\ell}$. Then the inequality $(D/\Sigma)^{1/3}\ell_x \lesssim \ell_y$ is satisfied most of the time. Therefore, the quantity $\varrho$ does not experience strong changes unlike $\ell_x$. The angle $\phi + \pi$ corresponds to inversion of vector $\boldsymbol{\ell}$ and thus is equivalent to $\phi$, so it will be enough to consider angle on the interval $-\pi/2 < \phi < \pi/2$, treating functions of $\phi$ (say, PDF of $\phi$) as periodic with a period $\pi$.

Substituting the expressions (9) into Eqs. (5) and (6) one concludes that due to the inequality $D \ll \Sigma$ (8) the only relevant component of the gradients of the random velocity is $\partial_x u_y$ [the detailed estimation of the neglected terms is presented in Appendix B; see Eqs. (B4)–(B6)]. Thus, we come to the stochastic system:

$$\partial_\tau \varrho = (1 + \zeta) \cos\phi \sin\phi, \tag{10}$$

$$\partial_\tau \phi = \zeta \cos^2\phi - \sin^2\phi, \tag{11}$$

where $\zeta(\tau) = \Sigma^{-1/3} D^{-2/3} \partial_x u_y$ and we have introduced the dimensionless time

$$\tau = \Sigma^{2/3} D^{1/3} t. \tag{12}$$

Further, we present all relations in terms of the dimensionless time $\tau$. The stated above scalings for the tumbling time and ratio $\ell_y/\ell_x$ are justified by the fact that the rescaling (9) and (12) carried out on their basis led to Eqs. (10) and (11) with coefficients of the order of unity and with noise of unit intensity, $\int_0^\infty \mathrm{d}\tau\, \langle \zeta(0)\zeta(\tau) \rangle = 1$.

In Eqs. (10) and (11), the regular and the random terms in right-hand sides are comparable, which was our motivation to introduce the parametrization (9). Note that Eq. (11) is a closed stochastic equation for the angle $\phi$, that is, a consequence of linearity of Eqs. (5) and (6). Thus, one can independently examine statistical characteristics of the angle $\phi$, based on Eq. (11). The variable $\varrho$ grows on average as time goes. The growth can be characterized by the dimensionless Lyapunov exponent $\lambda = \langle \partial_\tau \varrho \rangle$ [the dimensional Lyapunov exponent is $\tilde{\lambda} = \lambda (D\Sigma^2)^{1/3}$]. The averaging $\langle \cdot \rangle$ can be understood either over time or over the ensemble of $\zeta(\tau)$ realizations. One can also introduce the quantity $\omega = -\langle \partial_\tau \phi \rangle$, i.e., the dimensionless frequency of the tumbling processes, so tumblings occur an average of $\pi \Sigma^{2/3} D^{1/3} t/\omega$ times in the system for a large $t$. Both quantities, $\lambda$ and $\omega$, are of order of unity.

The general structure of the stochastic equations (10) and (11) enables one to find a relation for PDF of $\varrho$, $\Pi(\varrho)$ if the statistics of $\zeta$ is invariant under the time inversion. The property is assumed below. Then one relates the values of $\Pi(\varrho)$ for different signs of $\varrho$:

$$\Pi(-\varrho) = \exp(-2\varrho)\Pi(\varrho). \tag{13}$$

The relation (13) implies that at $\tau = 0$ the angle $\phi$ is fixed and that $\varrho = 0$. In Appendix A we present proof of (13) and indicate it is an expression of the Fluctuation Theorem [40,41].

Asymptotically, at $\tau \to \infty$, PDF $P(\phi)$ turns to a stationary distribution, if $\zeta$ has statistical properties homogeneous in time. As for PDF $\Pi(\varrho)$, it does not turn stationary at large times $\tau$ since $\varrho$ grows in average. Instead, in accordance with the theory of large deviations [42,43] at $\tau \gg 1$,

$$\Pi(\varrho) \propto \exp[-\tau S(\varrho/\tau)], \tag{14}$$

where $S(\xi)$ is the so-called Cramér (or entropy) function, which is convex. The function has a minimum at $\xi = \lambda$, that corresponds to the most probable realization $\varrho = \lambda\tau = \bar{\lambda}t$. Hence,

$$S'(\lambda) = 0, \tag{15}$$

where $S' \equiv dS/d\xi$. The normalization in Eq. (14) is determined by a close vicinity of the minimum point. We assume that $S(\lambda) = 0$. Then the normalized function

$$\Pi(\varrho) = \sqrt{\frac{S''(\lambda)}{2\pi\tau}} \exp[-\tau S(\varrho/\tau)] \tag{16}$$

is valid at $\tau \gg 1$.

The general law (13) leads to the relation

$$S(-\xi) = S(\xi) + 2\xi, \tag{17}$$

as follows from Eq. (14). Taking the derivative of the relation (17) one obtains

$$S'(-\xi) = -S'(\xi) - 2. \tag{18}$$

Substituting here $\xi = 0$, one obtains

$$S'(0) = -1. \tag{19}$$

Another consequence of Eq. (18) is $S'(-\lambda) = -2$, which can be established using Eq. (15).

It is instructive to introduce the Fourier transform of $\Pi(\varrho)$,

$$\widetilde{\Pi}(\eta) = \int d\varrho\, \exp(-\eta\varrho)\Pi(\varrho). \tag{20}$$

In the conventional Fourier transform $\eta$ is purely imaginary. However, we treat $\eta$ as an arbitrary complex number. In the limit $\tau \gg 1$ we can use the expression (14) and the integral (20) can be taken in the saddle point approximation. As a result, we find

$$\widetilde{\Pi}(\eta) \propto \exp[-\gamma(\eta)\tau], \tag{21}$$

where the function $\gamma(\eta)$ is related to the Cramér function $S(\xi)$ via the Legendre transform

$$S = \gamma - \eta\xi, \tag{22}$$

$$\partial_\eta\gamma = \xi, \quad \partial_\xi S = -\eta. \tag{23}$$

Solutions of Eqs. (22) and (23) correspond to real $\eta$. Taking into account the relation (18) one concludes that (17) is equivalent to

$$\gamma(\eta) = \gamma(2 - \eta). \tag{24}$$

Such symmetry was obtained, e.g., in [44] for their flow model with no mean component in periodic system.

The dimensionless Lyapunov exponent $\lambda$ is equal to the ratio $\xi = \varrho/\tau$, taken at the minimum of the Cramér function $S(\xi)$. As follows from Eq. (23), the minimum of $S$ is achieved at $\eta = 0$. Thus, we find from Eq. (23)

$$\lambda = \partial_\eta\gamma(0). \tag{25}$$

Since $\gamma$ is invariant under the transformation $\eta \to 2 - \eta$, the derivative of $\gamma$ over $\eta$ at $\eta = 1$ is equal to zero, $\partial_\eta\gamma(1) = 0$. Thus, we conclude from Eq. (22), that point $\eta = 1$ ($\varrho = \lambda\tau$) corresponds to the value $\xi = 0$.

### B. Random flow short correlated in time

To demonstrate the main features of the statistics of the Lagrangian trajectories, we examine the model where the random flow is short correlated in time. The model enables one to draw a number of analytical results [34]. In terms of our parametrization (9), the model is determined by the pair correlation function

$$\langle\zeta(\tau_1)\zeta(\tau_2)\rangle = 2\delta(\tau_1 - \tau_2), \tag{26}$$

where the factor in the right-hand side agrees with Eq. (7), considering passage to dimensionless $\tau$ [see below (12)].

We find, as a consequence of Eqs. (10) and (11) that the dimensionless Lyapunov exponent and the dimensionless frequency of the tumblings are equal to

$$\lambda = \langle\partial_\tau\varrho\rangle = \langle\cos\phi\sin\phi + \cos(2\phi)\cos^2\phi\rangle, \tag{27}$$

$$\omega = -\langle\partial_\tau\phi\rangle = \langle\sin^2\phi + \sin(2\phi)\cos^2\phi\rangle. \tag{28}$$

The first terms in the angular brackets in Eqs. (27) and (28) are related to the regular terms in the right-hand sides of Eqs. (10) and (11), whereas the second terms in the angular brackets are related to the terms with random variable $\zeta$ there. To find the latter contributions, one should find increments of $\varrho, \phi$, caused by $\zeta$, and take into account the increments in the right-hand sides of Eqs. (10) and (11) and then average the products of the increments and $\zeta$, using Eq. (26). The quantities (27) and (28) are expressed in terms of the statistics of the angle $\phi$ and can be calculated irrespective to the statistics of $\varrho$.

The Langevin equations (10) and (11) with the random variable governed by Eq. (26) enable one to establish the Fokker-Planck equations either for the PDF of the variable $\phi$ only or for the joint PDF of the variables $\varrho, \phi$. The corresponding technique is well known [45,46]. Therefore, we do not present the derivation of the Fokker-Planck equations, focusing on analyzing their solutions.

We begin with the Fokker-Planck equation for PDF of $\phi$, $P(\phi)$. The equation follows from Eqs. (11) and (26):

$$\partial_\tau P = \partial_\phi(\sin^2\phi\, P) + \partial_\phi[\cos^2\phi\, \partial_\phi(\cos^2\phi\, P)]. \tag{29}$$

Equation (29) has to be supplemented by the periodicity condition in terms of the angle $\phi$ and by some initial condition, e.g., the initial angle has some fixed value $\phi_0$, that leads to the initial $\delta$ function, $P = \delta(\phi - \phi_0)$ (continued periodically with the period $\pi$).

At $\tau \to \infty$ a stationary PDF of $\phi$ is achieved. The stationary solution $P_s$ of the equation (29) is written as

$$P_s(\phi) = \frac{N}{\cos^2\phi}\int_0^{\pi/2} \frac{d\psi}{\cos^2\psi} e^{[(\tan\phi - \tan\psi)^3 - \tan^3\phi]/3}, \tag{30}$$

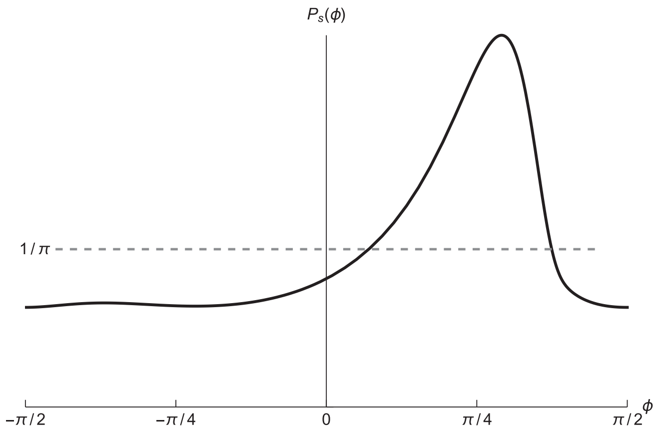


FIG. 1. Stationary PDF $P_s$ of the angle $\phi$ in the case of the short correlated in time flow fluctuations (26).

where the constant $N = 3^{5/6}/[2^{1/3}\sqrt{\pi}\Gamma(1/6)]$ is found from the normalization condition $\int d\phi\, P_s = 1$. The function $P_s$ is plotted in Fig. 1. Calculating numerically the averages (27) and (28) as integrals over $\phi$ with the weight $P_s(\phi)$, one obtains

$$\lambda = \frac{\pi N}{\sqrt{3}} \approx 0.36, \quad \omega = \pi N \approx 0.63. \tag{31}$$

The numerical values (31) are in agreement with the analysis given in Ref. [34]; see also Appendix B for more detailed comparison of our mathematical approach with the one used there.

Next, we turn to the joint PDF for $\varrho, \phi$, $\mathcal{P}(\tau, \varrho, \phi)$. The Fokker-Planck equation for the quantity is

$$\begin{aligned}\partial_\tau \mathcal{P} &= \partial_\phi(\sin^2\phi\, \mathcal{P}) - \partial_\varrho(\cos\phi \sin\phi\, \mathcal{P})\\ &\quad + \partial_\phi[\cos^2\phi\, \partial_\phi(\cos^2\phi\, \mathcal{P})] + \cos^2\phi \sin^2\phi\, \partial_\varrho^2 \mathcal{P}\\ &\quad + \partial_\phi(\cos^3\phi \sin\phi\, \partial_\varrho \mathcal{P}) + \cos\phi \sin\phi \partial_\phi(\cos^2\phi\, \partial_\varrho \mathcal{P}),\end{aligned} \tag{32}$$

as a consequence of Eqs. (10), (11), and (26). The PDF of $\varrho$, $\Pi(\varrho)$, can be found as

$$\Pi(\varrho) = \int_{-\pi}^{\pi} \frac{d\phi}{2\pi} \mathcal{P}(\varrho, \phi).$$

Note that no closed equation for $\Pi$ can be derived from Eq. (32).

We see that Eq. (32) is homogeneous in $\varrho$; it is a direct consequence of the linearity of the initial Eqs. (5) and (6). Therefore it is worth analyzing the equation in terms of the Fourier transform of $\mathcal{P}(\varrho)$. We introduce it by analogy with Eq. (20):

$$\tilde{\mathcal{P}} = \int d\varrho\, \exp(-\eta\varrho)\mathcal{P}, \tag{33}$$

where $\eta$ is some (complex) parameter. The analysis of the object $\tilde{\mathcal{P}}$ can be found in Appendix D. As a result, one can extract the function $\gamma(\eta)$ introduced by Eq. (21) and check directly the property (24).

The function $\gamma(\eta)$ can be calculated numerically. One can check that the value of $\lambda$, calculated in accordance with Eq. (25), coincides with one given by Eq. (31). Converting $\gamma(\eta)$ into $S(\xi)$ in accordance with Eqs. (22) and (23), one finds that in the minimum of $S(\xi)$, where $\xi = \lambda$,

$$S'' \approx 2.46, \quad S''' \approx -1.56. \tag{34}$$

The values (34) enable one to approximate the Cramér function $S$ near its minimum and to find the factor in Eq. (16).

## III. DECAY OF THE SCALAR

Here we consider decay of the passive scalar, which is described by the basic equation (1) with $f = 0$. We are interested in evolution of correlation functions of the passive scalar $\vartheta$ that have to be obtained by averaging over the statistics of the random flow. The statistical properties of $\vartheta$ appear to be extremely non-Gaussian at $\tau \gg 1$, where the dimensionless time $\tau$ is introduced by Eq. (12). We establish some features of the statistics.

Further we examine quantities obtained by averaging over an ensemble of the realizations of the initial distributions $\vartheta(0, \boldsymbol{r})$. We consider each one as the aggregation of similar blobs of the scalar fluctuations placed in the flow at $t = 0$, keeping zero total amount of scalar. Assuming the limit of their high concentration, i.e., overlapping of many blobs in each point, the value of $\vartheta(0, \boldsymbol{r})$ is a sum of large number of independent variables. Thus, as a consequence of the central limit theorem, the field $\vartheta(0, \boldsymbol{r})$ possesses Gaussian statistics with zero mean [30].

Let us introduce the object $\mathcal{F}(t, \boldsymbol{r}_1, \boldsymbol{r}_2)$ that is the product $\vartheta(t, \boldsymbol{r}_1)\vartheta(t, \boldsymbol{r}_2)$ averaged over the statistics of the initial values of $\vartheta$. To find any correlation function of the scalar, one should take the product $\vartheta(\boldsymbol{r}_1)\vartheta(\boldsymbol{r}_2)\dots$ and average it first over the initial statistics and then over the statistics of the random velocity field. The first step reduces the product $\vartheta(\boldsymbol{r}_1)\vartheta(\boldsymbol{r}_2)\dots$ to the product of $\mathcal{F}$ with some combinatoric factor in accordance with Wick theorem [47]. To make the second step, one should establish statistical properties of $\mathcal{F}$. We proceed to the problem.

If the ensemble of the initial values is statistically homogeneous in space, then $\mathcal{F}(t, \boldsymbol{r}_1, \boldsymbol{r}_2)$ is a function solely of the difference $\boldsymbol{r} = \boldsymbol{r}_1 - \boldsymbol{r}_2$, $\mathcal{F} = \mathcal{F}(t, \boldsymbol{r})$. In this case, one finds from Eq. (1) [see the derivation in Appendix C, Eq. (C1)]

$$\partial_t \mathcal{F} + \Sigma y \partial_x \mathcal{F} + (\partial_\beta u_\alpha) r_\beta \partial_\alpha \mathcal{F} = 2\kappa \nabla^2 \mathcal{F}, \tag{35}$$

where we have presumed like above (5) that the velocity field $\boldsymbol{v}$ of the flow is smooth and consists of the shear flow with the velocity $v_x = \Sigma y$ and the random flow with the velocity $\boldsymbol{u}$. Let us stress that the object $\mathcal{F}$ is a functional of the random variable $\partial_\beta u_\alpha$, entering Eq. (35).

By analogy with the analysis of the Lagrangian trajectories (see Sec. II A), we move to the rescaled coordinate $w = (D/\Sigma)^{1/3} x$ and the dimensionless time (12). Then one finds from Eq. (35)

$$\partial_\tau \mathcal{F} + y \partial_w \mathcal{F} + \zeta w \partial_y \mathcal{F} = r_\kappa^2 \partial_y^2 \mathcal{F}, \tag{36}$$

where $\zeta = \Sigma^{-1/3} D^{-2/3} \partial_x u_y$. We have kept in Eq. (36) the only relevant component of the random velocity gradient, $\partial_x u_y$, the main derivative $\partial_y$ in the Laplacian, and have introduced the diffusive scale

$$r_\kappa = (2\kappa)^{1/2} \Sigma^{-1/3} D^{-1/6}. \tag{37}$$

The Batchelor scale $r_\kappa$ is assumed to be much smaller than characteristic scales of the initial scalar field and of the forcing one.

It is instructive to examine a Gaussian shape of $\mathcal{F}$: such a profile of spatial distribution, formed by the initial statistics, is preserved in Eq. (35). We suppose that initially $\mathcal{F}(0,\boldsymbol{r}) = \exp(-r^2/L^2)$, where $L$ is the characteristic initial scale. Then the quantity $\mathcal{F}$ at any time $t$ is expressed as

$$\mathcal{F} = \frac{\sqrt{\det \hat{\Lambda}}}{\sqrt{\det \hat{\Lambda}|_{t=0}}} \exp(-\Lambda_{\alpha\beta} b_\alpha b_\beta), \tag{38}$$

where the $\boldsymbol{b}$ is a coordinate vector in rescaled space, $b_\alpha = (w, y)$, the symmetric matrix $\hat{\Lambda}$ is a function of time, which dynamics is consistent with Eq. (36), and we have normalized the scalar intensity so $\mathcal{F}(0,0) = 1$. The time-dependent factor at the exponent in Eq. (38) is determined by the fact that total amount of the passive scalar $\int d^2b\,\vartheta$ is conserved in time according to Eq. (36); see Ref. [48].

We use the following parametrization of the matrix $\hat{\Lambda}$ figuring in Eq. (38):

$$\hat{\Lambda} = \begin{pmatrix} c & -s \\ s & c \end{pmatrix} \begin{pmatrix} L_+^{-2} & 0 \\ 0 & L_-^{-2} \end{pmatrix} \begin{pmatrix} c & s \\ -s & c \end{pmatrix}, \tag{39}$$

where $c = \cos\phi$, $s = \sin\phi$. The eigenvalues of the matrix (39) are $L_+^{-2}, L_-^{-2}$, where $L_\pm$ can be interpreted as sizes of the scalar blob in $\boldsymbol{b}$ space. Therefore the factor $\sqrt{\det \hat{\Lambda}}$ entering Eq. (38) is equal to

$$\sqrt{\det \hat{\Lambda}} = (L_+ L_-)^{-1}, \tag{40}$$

i.e., the inverse area occupied in $\boldsymbol{b}$ space by the blob. In accordance with Eqs. (38) and (39), for the initial profile $\propto \exp(-r^2/L^2)$, we have $\phi(0) = \pi/2$,

$$L_+(0) = L, \quad L_-(0) = L_\star, \quad L_\star = (D/\Sigma)^{1/3} L. \tag{41}$$

Thus, initially $L_+ \gg L_-$. We will see that the ratio $L_+/L_-$ typically grows with time and will neglect very rare events when the ratio becomes of order unity. Thus, we assume $L_+ \gg L_-$ is fulfilled further all the time.

Substituting the parametrization (39) into Eq. (38) and then using Eq. (36), one finds the equations for the angle $\phi$ and the parameters $L_\pm$. In the limit $L_+ \gg L_-$ one reproduces Eq. (11) for the angle $\phi$ and the equations for $L_\pm$ are

$$\partial_\tau \ln L_+ = \cos\phi\, \sin\phi\, (1+\zeta), \tag{42}$$

$$\partial_\tau \ln L_- = -\cos\phi\, \sin\phi\, (1+\zeta) + 2\frac{r_\kappa^2}{L_-^2}\cos^2\phi. \tag{43}$$

Our interest is statistics of the solutions of Eqs. (42) and (43) at times $\tau \gg 1$ where PDF of the angle $\phi$ achieves stationary distribution.

Equation (42) coincides with Eq. (10) for $\varrho$. Consequently, $\ln(L_+/L)$ has the same statistical properties as $\varrho$; see Sec. II. Typically, $\ln(L_+/L)$ is estimated as $\lambda\tau$. As to the quantity $L_-$, its statistical properties depend on its value. If $L_- \gg r_\kappa$ then the last term in Eq. (43) is irrelevant, and we find $L_- = LL_\star/L_+$. Therefore $L_-$ typically diminishes exponentially as time goes. If $L_-$ reaches $r_\kappa$, then its statistical properties become stationary, and the estimate $L_- \sim r_\kappa$ is valid.

The duration of the first (advective or diffusionless) stage is

$$\tau_\kappa = \frac{1}{\lambda}\ln\frac{L_\star}{r_\kappa} = \frac{1}{2\lambda}\ln\frac{DL^2}{\kappa}. \tag{44}$$

We assumed here

$$DL^2/\kappa \gg 1. \tag{45}$$

More precisely, below we assume that $\ln(DL^2/\kappa)$ is large, so $\tau_\kappa \gg 1$. Otherwise, if $DL^2/\kappa \lesssim 1$, the mixing process is determined only by the mean shear flow $\Sigma$ and the molecular diffusion; the limit $\Sigma L^2/\kappa \gg 1$ was considered in [31]. Inequality (45) implies that at scale $L$ the influence of the molecular diffusion is weaker than both the influence of shear flow and the stirring acceleration by the flow's random component. Note that the limit of the large Péclet number $\mathrm{Pe} = L^2/r_\kappa^2 \sim (D\Sigma^2)^{1/3}L^2/\kappa \gg 1$ in our system does not provide a sufficient criterion. The amplitude (40) remains constant at the advective stage and behaves $\propto L_+^{-1}$ at the second (diffusive) stage. Since initially $L_+L_- = LL_\star$ we conclude that $L_+ \sim LL_\star/r_\kappa$ in the transition region between the stages, which leads to the condition

$$\ln(L_+/L) > \lambda\tau_\kappa \tag{46}$$

at the diffusive stage.

Let us stress here that the only term $\partial_x u_y$ taken into account in (6) produces the leading contribution into the stirring process. As a result of joint action of the constant shear and this random component, the Lyapunov exponent becomes nonzero. Indeed, other models with random shear flow having the only nonzero $x$-velocity component $v_x(t, y)$ lead to only algebraic in time divergence of Lagrangian trajectories over long times, i.e., to zero Lyapunov exponent. This concerns, e.g., [49], where $v_x(t, y)$ contains a part which is random in both time and space. Within the model, a finite Lyapunov exponent was obtained in Ref. [50], which, however, tends to zero as the system size grows. One more example is an extended model [51] where the random component is taken into account only in $\partial_z u_x$ and $z$ is the third coordinate.

### A. Single-point statistics

Let us analyze moments of the passive scalar that are single-point means $\langle|\vartheta|^{2\alpha}\rangle$. To find the moments we use the expression

$$\langle|\vartheta|^{2\alpha}\rangle = C_\alpha\langle[\mathcal{F}(t,\mathbf{0})]^\alpha\rangle, \tag{47}$$

where $C_\alpha = 2^\alpha\Gamma(\alpha+1/2)/\sqrt{\pi}$. The expression (47) is a consequence of the initial Gaussian statistics of $\vartheta(0,\boldsymbol{r})$. Although the expression (47) implies a particular statistics of initial values of $\vartheta$, the results concerning the behavior of the moments at large times $\tau \gg 1$ are universal, because they are determined by the flow statistics.

Substituting the expression (38) with the factor (40) into Eq. (47) one arrives at the following expression for the moments:

$$\langle|\vartheta|^{2\alpha}\rangle = C_\alpha\langle(L_+L_-/LL_\star)^{-\alpha}\rangle. \tag{48}$$

Thus, the passive scalar moments can be calculated using the statistical properties of $L_\pm$ established above. At the advective stage, where $\tau < \tau_\kappa$, the product $L_+L_-$ remains constant and the mean $\langle|\vartheta|^{2\alpha}\rangle$ is independent of time $\tau$. For the case of statistically isotropic turbulence, the advective stage is observed both in experiments for large Schmidt numbers [52] and in numerical simulations [53]. Qualitatively, the spatial distribution of the scalar is expressed via stretched and folded blobs. Both stretching and folding are results of stirring by flow only, so the scalar amplitude inside the blobs *stays the same as at the initial moment.* In other words, the volume occupied by each blob remains unchanged at the advective stage.

Further we focus on the subsequent stage: at $\tau > \tau_\kappa$ the diffusion becomes relevant. This is the mixing stage, when the area occupied by a blob grows exponentially with time by means of its largest dimension stretching, while the smallest transverse size cannot diminish below the diffusion scale. This increase of the blob's area leads to the decrease of the scalar amplitude inside it. Calculating the scalar statistics, one should also take into account that the number of blobs overlapping in a single point grows with time at the stage. Let us start with calculations. The diffusive stage corresponds to the inequality (46), which is equivalent to the requirement $\varrho > \lambda\tau_\kappa$. Here we estimate the lowest blob dimension $L_-$ as the diffusion scale $r_\kappa$ so the ratio $L_\star/L_- \sim \exp(\lambda\tau_\kappa)$ in (48) according to (44), whereas $L_+$ is determined by PDF (16) with $\varrho = \ln(L_+/L)$ so its typical value depends on $\alpha$ and $\tau$. Now one can write for (48)

$$\langle|\vartheta|^{2\alpha}\rangle \sim \int_{\lambda\tau_\kappa}^{\infty} d\varrho \exp\left[-\alpha(\varrho - \lambda\tau_\kappa) - \tau S(\varrho/\tau)\right], \quad (49)$$

where we have exploited Eq. (16), omitting its pre-exponential factor as well as $C_\alpha$ in (48) since this is a multiplier with relatively weak dependence on $\alpha$.

In the case $0 < \alpha < 1$ at large enough times, the integral (49) for the moment $\langle|\vartheta|^{2\alpha}\rangle$ is determined by the saddle point, which is the solution of

$$\alpha + S'(\xi) = 0, \qquad \varrho = \xi\tau. \quad (50)$$

The value of $\xi$ found in accordance with Eq. (50) belongs to the interval $0 < \xi < \lambda$, since $S'(\lambda) = 0$ and $S'(0) = -1$; see Sec. II A. To ensure the saddle point lies in the integration interval, one should require $\varrho > \lambda\tau_\kappa$, so time $\tau$ should satisfy the inequality $\tau > \lambda\tau_\kappa/\xi$. Now, we substitute $\rho$ from (50) into (49) and obtain

$$\langle|\vartheta|^{2\alpha}\rangle \sim \exp[\alpha\lambda\tau_\kappa - \gamma(\alpha)\tau], \quad (51)$$

where $\gamma(\eta)$ is found in accordance with the Legendre transform (22) and (23). Since $\xi < \lambda$, there is an intermediate time asymptotic $\tau_\kappa < \tau < \lambda\tau_\kappa/\xi$ within the diffusion stage: in this time interval, the integral (49) is determined by the smallest possible value $\varrho = \lambda\tau_\kappa$ under the condition that the diffusion does not affect scalar dynamics. So we find

$$\langle|\vartheta|^{2\alpha}\rangle \sim \exp[-\tau S(\lambda\tau_\kappa/\tau)]. \quad (52)$$

Note that (52) is independent of $\alpha$ (up to the dropped $C_\alpha$) since it gives the probability that $\varrho$ process reaches fixed value $\lambda\tau_\kappa$ just in time $\tau$ and has been in advective stage of dynamics up to that moment. For such random flow velocity realizations, the scalar amplitude in each blob is equal to its initial value, whose order is of unity.

If $\alpha > 1$, the condition $\varrho > 0$ is violated for the saddle point, determined by Eq. (50), for any $\tau$. Indeed, the equation leads to $\xi < 0$ and, consequently, to $\varrho < 0$. In this situation, again, the integral (49) is determined by the value $\varrho = \lambda\tau_\kappa$, which is the largest possible one under the condition that the diffusion does not play any role in the scalar dynamics. We conclude that the relation (52) is correct at any time $\tau > \tau_\kappa$ for $\alpha > 1$.

Further, we reformulate the results for the one-point moments in terms of the one-point PDF $\mathcal{P}_\vartheta$. At a fixed realization of the velocity, the PDF of the scalar is Gaussian,

$$\widetilde{\mathcal{P}}_\vartheta(\vartheta, \varrho) = \frac{1}{\sqrt{2\pi\mathcal{F}(t, \mathbf{0})}} \exp\left(-\frac{\vartheta^2}{2\mathcal{F}(t, \mathbf{0})}\right). \quad (53)$$

Until the time $\tau$ reaches the diffusion time, $\tau < \tau_\kappa$, the object $\mathcal{F}(t, \mathbf{0}) = 1$ for most probable velocity realizations, so the scalar PDF $\mathcal{P}_\vartheta(\vartheta)$ coincides with the initial one. After that at times $\tau > \tau_\kappa$, the averaging over the velocity statistics leads to

$$\mathcal{P}_\vartheta = \int_{\lambda\tau_\kappa}^{\infty} d\varrho\, \widetilde{\mathcal{P}}_\vartheta(\vartheta, \varrho)\, \Pi(\varrho) \sim \frac{1}{|\vartheta|} \exp[-\tau S(\varrho_*/\tau)], \quad (54)$$

where the scalar intensity is assumed not to exceed the characteristic initial value, $|\vartheta| \lesssim 1$, and the optimal velocity fluctuation is determined by $\varrho_* = \lambda\tau_\kappa - 2\ln|\vartheta|$. The obtained PDF (54) corresponds to the relation (49) and is applicable for the intensities $|\vartheta|$ which are greater than the scalar intensity at the most probable velocity realizations, $|\vartheta| > e^{-\lambda(\tau-\tau_\kappa)/2}$. In this region the PDF can be characterized by its logarithmic derivative $\partial_\vartheta \ln \mathcal{P}_\vartheta = (2S'(\varrho_*/\tau) - 1)/\vartheta$. At large times it results in power-law dependence on $|\vartheta|$ with exponent $[2S'(0) - 1] = -3$ up to the scale of the scalar maximum possible amplitude $|\vartheta| \sim 1$. This means that all moments with $\alpha \geqslant \alpha_c$, $\alpha_c = 1$ are determined by the peaks in the scalar intensity. Such peak events correspond to the nontypical flow realizations, where the $\varrho$ process reaches fixed value $\lambda\tau_\kappa$ just in time $\tau$, so the lowest dimension of the scalar blob was not affected by the molecular diffusion during all the observation time up to $\tau$.

In the case of the isotropic turbulent flow, the critical value $\alpha_c = 1$ for the 2D model of short-correlated velocity gradient in time [29] as well. The corresponding algebraic tail of PDF $\mathcal{P}_\vartheta \propto |\vartheta|^{-3}$ had been confirmed by numerical simulation [53]. Analytically, the single-point statistics (51) and (52) was established in [28,29]; before that, the asymptotic (51) was separately found for scalar variance $\langle\vartheta^2\rangle$ in [54].

The results are obtained within the Lagrangian stretching theory that has limiting factors. In an experiment or a numerical simulation, the significant limitation of Eq. (52) applicability is lack of statistical data for sampling that inevitably raises at large times. The right-hand side of the expression means probability of the flow realizations preserving the $L_-$ dimension no lower than diffusion one. It decreases in time exponentially, so one needs an increasingly large statistical population in order to restore the tail of theoretical distribution (16) from the data. Instead of this at large times, due to the data amount being finite, the restored empirical distribution is determined on the basis of the most probable flow realizations that provide $\rho \sim \tau$. Such collapse to narrow distribution was proposed in Ref. [55], leading to linear dependence $\gamma(\alpha)$ at $\alpha > \alpha_c$, which authors observed; see also [53]. We can also address to the review [56] for extensive discussion of the single-point scalar statistics in a random smooth flow for the decay problem.

### B. Pair correlation function

The pair correlation function $F$ of the passive scalar $\vartheta$ can be written as the average

$$F(t, \boldsymbol{r}) = \langle \mathcal{F}(t, \boldsymbol{r}) \rangle. \tag{55}$$

We suppose that the initial statistics leads to the Gaussian initial spatial form of $\mathcal{F}$, so it has the form as in Eq. (38) at any time. The parametrization (39) implies that averaging in Eq. (55) is performed over the statistics of $\phi, L_+, L_-$, examined above.

Passing to polar coordinates in the rescaled space:

$$w = (D/\Sigma)^{1/3} x = b\cos\psi, \quad y = b\sin\psi, \tag{56}$$

we find for the argument in the exponent in Eq. (38)

$$\Lambda_{\alpha\beta} b_\alpha b_\beta = b^2 L_+^{-2} \cos^2(\phi - \psi) + b^2 L_-^{-2} \sin^2(\phi - \psi). \tag{57}$$

Thus, if $b \ll L_-$ then the quantity (57) is much less than unity, and the pair correlation function is reduced to the second moment of $\vartheta$ examined in Sec. III A. Hence, below we examine the case $b \gg L_-$. Note that the criterion depends on time at the advective stage of the passive scalar evolution and is reduced to $b \gg r_\kappa$ at the diffusive stage.

If $b \gg L_-$, then the quantity (57) has a deep minimum at $\phi = \psi$. Correspondingly, $\exp(-\Lambda_{\alpha\beta} b_\alpha b_\beta)$ has a sharp peak at this point. Thus, averaging over $\phi$ statistics brings us to the factor proportional to the peak's width,

$$F \sim \left\langle \frac{L_\star L}{b L_+} \exp(-b^2 L_+^{-2}) \right\rangle_+, \tag{58}$$

as a consequence of Eqs. (38) and (40). Remarkably, $L_-$ falls out of consideration and we stay with averaging solely over the statistics of $L_+$ in Eq. (58). The factor in the proportionality law (58) depends on the angle $\psi$. Its exact value is determined by details of the $\phi$ distribution and, consequently, is not universal, since that depends on the statistics of $\zeta$ (11). As we have implemented the rescaling (9) and (56), the distribution is anticipated to be nearly isotropic; an example for a short correlated case is given in Fig. 1. For this reason we focus on the dependence of the pair correlation function on the length $b$.

The average in (58) can be written as the integral over $\varrho = \ln(L_+/L)$ with the weight (16). Due to the strong dependence on $\varrho$ of $\exp(-b^2 L_+^{-2})$, the last factor restricts the integration region to $\varrho > \ln(b/L)$, so we arrive at

$$F \sim \frac{L_\star}{b} \int_{\varrho_{\min}}^{\infty} d\varrho \exp\left[-\varrho - \tau S(\varrho/\tau)\right] \tag{59}$$

if $b \gg L_-$ and $\varrho_{\min} = \max(\ln(b/L), \ln\sqrt{L_\star/L})$. The integral above is of the same type as in Sec. III A and can be analyzed similarly.

If $\ln(b/L) < 0$ ($b \ll L$) then the integral in Eq. (59) is determined by the saddle point $\varrho = 0$ in accordance with (19), and we obtain

$$F \sim \frac{L_\star}{b} \exp\left[-\tau S(0)\right]. \tag{60}$$

If $\ln(b/L) > 0$ ($b \gg L$) then the integral in Eq. (59) is determined by the allowed minimal value $\rho_{\min} = \ln(b/L)$ of $\varrho$, and we find

$$F \sim \frac{L L_\star}{b^2} \exp\left[-\tau S\left(\frac{\ln(b/L)}{\tau}\right)\right]. \tag{61}$$

Note that the function (61) diminishes monotonically as $b$ increases. Indeed, the derivative

$$\frac{\partial \ln F}{\partial \ln(b/L)} = -2 - S'\left(\frac{\ln(b/L)}{\tau}\right)$$

is negative since $S'(\xi) > -1$ for $\xi > 0$.

The derivation above, as mentioned earlier, implies the inequality $b \gg L_-$. It is correct if $b$ is much larger than the initial value of $L_-$ (41), i.e., $b \gg L_\star$. However, if $r_\kappa \ll b \ll L_\star$ then the optimal value of $L_-$ is $L_- \sim b$ that violates the condition of the sharp peak in averaging over $\phi$ statistics, so the latter just produces a factor of order unity. Since $L_- \sim b \gg r_\kappa$, the diffusion term in Eq. (43) is irrelevant, and we come to

$$L_+ = L L_\star / L_- \sim L L_\star / b.$$

Therefore, providing times are large enough, $\lambda\tau > \ln(L_\star/b)$, we conclude

$$F \sim \exp\left[-\tau S\left(\frac{\ln(L_\star/b)}{\tau}\right)\right]. \tag{62}$$

Otherwise, $\lambda\tau < \ln(L_\star/b)$ means $L_- \gg b$, which brings us to the mean square $F = 1$.

Let us return to the fact that the pair correlation function does not depend on the diffusion coefficient above the Batchelor scale $r_\kappa$; see (58). Hence, it is determined only by the statistics of Lagrangian trajectories. As it is demonstrated in Appendix C, there is a relation between the joint PDF $\mathcal{P}(\tau, \varrho, \phi)$ (32) and pair correlation function $F$ (55) in this region: $F \propto \mathcal{P}/b^2$. Dependency (61) agrees with this relation as well as with (60) and (62) if one employs symmetry (17) and the Cramér function expansion near zero. The relation between the Cramér function and the pair correlation function $F$ *can be thus considered as general* and be employed as a way to extract the Cramér function via experimental measurements of passive scalar spatial statistics.

### C. Higher order correlation functions

The pair correlation function $F$ does not reflect the presence of folding in the passive scalar spatial distribution. This is due to the function being also the result of averaging over angle, which makes the statistics near-isotropic. The folded structure can be revealed with the aim of higher-order correlation functions. As was demonstrated in Ref. [57], higher order correlation functions of the passive scalar $F_{2n}(\boldsymbol{r}_1, \ldots, \boldsymbol{r}_{2n})$ in the Batchelor regime have sharp maxima in collinear geometry where the points $\boldsymbol{r}_1, \ldots, \boldsymbol{r}_{2n}$ are separated in pairs with parallel differences. One can think that the folded structure is caused by overlapping of scalar blobs which are strongly stretched. The collinear geometry provides the vectors in each pair can be covered simultaneously by a blob during the averaging over angle.

Let us consider such collinear geometry. It corresponds to the following leading contribution to the $2n$-th correlation function:

$$F_{2n} = \langle \mathcal{F}(b_1, \psi) \dots \mathcal{F}(b_n, \psi) \rangle, \tag{63}$$

where $\mathcal{F}$ are determined by Eqs. (38), (40), and (57) and the angular brackets mean averaging over the statistics of $\phi, L_+, L_-$.

For definiteness, we consider the case $b \gg L$ where $b^2 = b_1^2 + \dots + b_n^2$. Then we obtain

$$F_{2n} \sim \int_{\ln(b/L)}^{\infty} \frac{L_\star^n d\varrho}{bL_-^{n-1}} \exp\left[-n\varrho - \tau S(\varrho/\tau)\right] \tag{64}$$

instead of Eq. (59). The integral in Eq. (64) is determined by the lower limit, i.e., $L_+ \sim b$. If $b \ll LL_\star/r_\kappa$ then we obtain the same proportionality law as in Eq. (61), $F_{2n} \sim F$, since the optimal velocity fluctuation corresponds to the suppressed diffusion so $L_+L_- = LL_\star$. Otherwise, at $b \gg LL_\star/r_\kappa$, one has $L_- \sim r_\kappa$ and

$$F_{2n} \sim \frac{(LL_\star)^n}{r_\kappa^{n-1} b^{n+1}} \exp\left[-\tau S\left(\frac{\ln(b/L)}{\tau}\right)\right]. \tag{65}$$

In both cases, the correlation function $F_{2n}$ much exceeds its naive expectation, $F_{2n} \gg F^n(b/\sqrt{n})$ for moderate $n$.

## IV. CONTINUOUS FORCING OF SCALAR

Now we consider the problem where fluctuations of passive scalar field $\vartheta$ are excited in the system for a long time via random supply $f$; see Eq. (1). If its correlation time is shorter than scale $\Sigma^{-2/3}D^{-1/3}$ of scalar evolution, excitation can be represented as an aggregation of statistically independent contributions (blobs), which results in Gaussian statistics of $\vartheta$ before averaging over the flow statistics, as for the decaying case; see Sec. III.

By analogy with the decaying case we introduce the object $\mathcal{F}(t, \boldsymbol{r}_1, \boldsymbol{r}_2)$ that is the product $\vartheta(t, \boldsymbol{r}_1)\vartheta(t, \boldsymbol{r}_2)$ averaged over the statistics of the forcing $f$ at a given random velocity $\boldsymbol{u}$. Since the statistics of $\vartheta$ is Gaussian (before averaging over the statistics of $\boldsymbol{u}$), any product $\vartheta(t, \boldsymbol{r}_1) \dots \vartheta(t, \boldsymbol{r}_{2n})$ averaged over the statistics of $f$ is expressed via the products of $n$ factors $\mathcal{F}$ in accordance with Wick theorem [47].

For definiteness, we assume that the forcing $f$ is short correlated in time. Then its statistics is determined by the pair correlation function

$$\langle f(t_1, \boldsymbol{r}_1) f(t_2, \boldsymbol{r}_2) \rangle = \delta(t_1 - t_2)\Theta(\boldsymbol{r}_1 - \boldsymbol{r}_2). \tag{66}$$

The expression (66) implies homogeneity of $f$ statistics in space and time. We assume that $\Theta$ has the characteristic scale $L$ much smaller than the correlation length of the flow. However, $L$ is assumed to be much larger than the diffusion length $r_\kappa$ (37).

In our case $\mathcal{F}(t, \boldsymbol{r}_1, \boldsymbol{r}_2)$ is a function solely of the difference $\boldsymbol{r} = \boldsymbol{r}_1 - \boldsymbol{r}_2$, as a consequence of spatial homogeneity of the forcing statistics. One finds from Eqs. (1) and (66)

$$\partial_t \mathcal{F} + \Sigma y \partial_x \mathcal{F} + x(\partial_x u_y)\partial_y \mathcal{F} = 2\kappa \nabla^2 \mathcal{F} + \Theta(\boldsymbol{r}). \tag{67}$$

Here, as previously, we have kept the only relevant gradient of the random velocity $\boldsymbol{u}$, $\partial_x u_y$. One can also substitute $\nabla^2 \to \partial_y^2$ in Eq. (67).

The solution of (67) can be carried out from previous calculations for the decay problem in Sec. III. Indeed, one can take solution (35) with the initial condition $\mathcal{F}(t, \boldsymbol{r}) = \Theta(\boldsymbol{r})$ at a preceding time moment and consider its evolution till the current time—so we get the contribution from one time moment of forcing $t$, the result will be obtained by integration over time interval of $f$ activity. In sense of our model, each blob brought into system has been evolving from that moment in flow and $\mathcal{F}$ is a cumulative result of all blobs over all time till now, while they could have been brought.

As for the decay case, it is instructive to analyze the Gaussian profile of the forcing correlation function $\Theta \propto \exp(-r^2/L^2)$. Then we find the solution of Eq. (67) in the large time limit:

$$\mathcal{F}(\boldsymbol{r}) = \int_0^\infty d\tau \, \frac{LL_\star}{L_+L_-} \exp(-\Lambda_{\alpha\beta} b_\alpha b_\beta), \tag{68}$$

where the matrix $\hat{\Lambda}$ is determined by Eq. (39). The quantities $\phi, L_+, L_-$ are introduced in Sec. III, and their statistical properties are established there as well.

### A. Single-point statistics

Here we consider moments of the passive scalar, i.e., the single-point means $\langle |\vartheta|^{2\alpha} \rangle$. As in the decaying case, before averaging over the flow fluctuations the passive scalar possesses Gaussian statistics. Therefore at a given flow the moment is equal to $C_\alpha(\mathcal{F})^\alpha$ where $C_\alpha$ is the same as in (47), $\mathcal{F}$ is a value of (68) at the origin, and $\boldsymbol{r} = 0$. Thus, the moment is equal to

$$\langle |\vartheta|^{2\alpha} \rangle = C_\alpha \langle (\mathcal{F})^\alpha \rangle. \tag{69}$$

At the condition $L_\star \gg r_\kappa$ the main contribution to the single-point $\mathcal{F}$ is caused by the first stage where the product $L_+L_-$ remains constant; the contribution is proportional to the duration of the advective stage $\tau$. Taking into account the probability of the event where $L_-$ reaches $r_\kappa$, we find from Eq. (69)

$$\langle |\vartheta|^{2\alpha} \rangle \sim C_\alpha \tau^\alpha \exp\left[-\tau S\left(\frac{\ln(L_\star/r_\kappa)}{\tau}\right)\right]. \tag{70}$$

Here the parameter $\tau$ is a subject of optimization.

At moderate $\alpha$ the maximum of the expression (70) is achieved where the Cramér function $S$ is minimal, i.e., at $\tau = \ln(L_\star/r_\kappa)/\lambda$. This obviously leads to the Gaussian single-point statistics of $\vartheta$. In the case the moments (69) are expressed via the second moment as follows:

$$\langle |\vartheta|^{2\alpha} \rangle = C_\alpha \langle \vartheta^2 \rangle^\alpha, \tag{71}$$

$$\langle \vartheta^2 \rangle = \frac{\Theta(0)}{\bar{\lambda}} \ln(L_\star/r_\kappa), \tag{72}$$

where $\bar{\lambda}$ is the dimensional Lyapunov exponent and $\Theta(0)$ is the scalar variance production rate. The result corresponds to one established in Ref. [58].

However, for large exponents, $\alpha \gtrsim \ln(L_\star/r_\kappa)$, the moments strongly deviate from the relation (71). Optimizing the expression (70) over $\tau$, one finds the condition $\gamma\tau = \alpha$ where $\gamma$ is determined as Legendre transform of $S$; see Eqs. (22) and (23). If $\alpha \ll \ln(L_\star/r_\kappa)$ then $\gamma$ is small and we return to Eq. (71). If $\alpha \gg \ln(L_\star/r_\kappa)$ then $\alpha = S(0)\tau$, so $\tau \gg \ln(L_\star/r_\kappa)$ as well. The regime corresponds to the exponential tail of PDF for $\vartheta$, $\exp(-\theta/\theta_0)$, where $\theta_0^2 = \Theta(0)(D\Sigma^2)^{-1/3}/S(0)$.

### B. Pair correlation function

Now we move on to examine correlation functions of the passive scalar $\vartheta$. We begin with the pair correlation function. As in the decay problem, the averaging over flow statistics is required: $F(\boldsymbol{r}) = \langle \mathcal{F}(\boldsymbol{r})\rangle$. In the limit of long-lasting supply $F(\boldsymbol{r})$ is independent of time, as a consequence of homogeneity of the forcing statistics in time. Therefore, we examine $\langle \mathcal{F}(\boldsymbol{r})\rangle$ where $\mathcal{F}(\boldsymbol{r})$ is given by Eq. (68).

For $b \ll r_\kappa$ we return to the second moment (72). Let us consider the opposite case, $r_\kappa \ll b \ll L_\star$. Then the same logic as for the second moment does work. The main contribution to $F$ is produced by the advective stage where the product $L_+L_-$ is a constant and the exponent in Eq. (68) can be substituted by unity. The regime is finished where $L_-$ reaches $b$. The time of the process is proportional to the corresponding logarithm, and we obtain an expression that is independent of the $\boldsymbol{b}$ vector's direction:

$$F = \frac{\Theta(0)}{\lambda\!\!\!^{-}}\ln(L_\star/b). \tag{73}$$

Formulas (72) and (73) are analogous to the well-known result for the isotropic case, and (73) describes the Batchelor cascade of passive scalar variations towards smallest scales [1,7,8] in coordinate representation. The dependence (73) can be directly obtained by solving the equation for the pair correlation function $F$, as shown in Appendix C.

For $b \gg L_\star$, so $L_-/b \ll 1$ at any time, after angle averaging we obtain similar to (59) the expression

$$F \sim \frac{L_\star}{b}\int_0^\infty d\tau \int_{\ln(b/L)}^\infty d\varrho \exp\left[-\varrho - \tau S(\varrho/\tau)\right]. \tag{74}$$

If $b \ll L$, i.e., $\ln(b/L) < 0$, the integral over $\tau$ is determined by $\tau \sim 1$, hence the approximation (74) is, strictly speaking, incorrect. However, one can assert that $F \sim (\Theta(0)/\lambda\!\!\!^{-})L_\star/b$ in the region due to the averaging over angles. If $\ln(b/L) > 0$ ($b \gg L$), then $\varrho > 0$ in the whole region of the integration. Then the integral over $\tau$ in Eq. (74) is determined by a narrow vicinity of $\tau = \varrho/\lambda$. After integration over $\tau$ the integration over $\varrho$ will be determined by the lower limit, and we find $F \sim (\Theta(0)/\lambda\!\!\!^{-})LL_\star/b^2$. The dependence is in agreement with the stationary solution of Eq. (C4) for the pair correlation function $F$; see Appendix C and in particular (C3).

### C. Higher order correlation functions

Next, we continue our examination to high-order correlation functions $F_{2n}$. They can be represented as the sum of the $n(n-1)/2$ products of $\mathcal{F}$ in accordance with Wick theorem [47], where each product in the sum should be averaged over the statistics of the random flow. Below we analyze a product in the sum.

In situation where all the separations between the points are much smaller than $L_\star$, the main contribution to the average of the product of $n$ multipliers $\mathcal{F}$ is related to the advective stage. Each $\mathcal{F}$ gives the factor determined by the duration of the regime where the product $L_+L_-$ remans constant and there is no suppression related to averaging over the statistics of the angle. For moderate $n$ the evolution of $L_-$ is determined by the typical processes: $\ln(L_\star/L_-) = \lambda\tau$. Then the duration for each $\mathcal{F}$ is proportional to the same logarithm (73) and average of the product of $\mathcal{F}$'s is reduced to the product of the averages. In other words, we arrive to the Gaussian statistics for moderate number $n$ of multipliers in product, where $F_{2n}$ can be expressed via $F$ in accordance with Wick theorem [47].

However, if $n$ is large enough, the main contribution to $F_{2n}$ is related to rare events in which the $L_-$ decrease is much slower than typically, as it was for high moments of $\theta$. In this case the value of $F_{2n}$ is determined by the duration of the event and is insensitive to the logarithms. We conclude that in this limit $F_{2n}$ coincides with the moment $\langle(\vartheta)^{2n}\rangle$; see Sec. IV A. This non-Gaussian regime implies that $n$ exceeds logarithms for each pair correlation function (73) in the product. Note that the regime can be realized for lower $n$ than in the one-point moments case, since logarithms for the correlation functions are smaller than $\ln(L_\star/r_\kappa)$.

In the limit where separations are much larger than $L$, the situation is more complicated. As was demonstrated in Ref. [57], higher order correlation functions of the passive scalar $F_{2n}(\boldsymbol{r}_1,\dots,\boldsymbol{r}_{2n})$ in the Batchelor regime have sharp maxima in collinear geometry where the points $\boldsymbol{r}_1,\dots,\boldsymbol{r}_{2n}$ are separated into pairs with parallel differences. Let us consider such collinear geometry. It corresponds to the average (63), where now $\mathcal{F}$ is determined by Eq. (68). Averaging over the statistics of the angle $\phi$, one finds the extra factor $(L_-/b)\exp(-b^2L_+^{-2})$, as in Eq. (64), where $b^2 = b_1^2 + \cdots + b_n^2$. The factor $\exp(-b^2L_+^{-2})$ implies that the effective minimum value of $\varrho = \ln(L_+/L)$ is $\ln(b/L)$. The integral over $\varrho$ is gained near its minimum value. Therefore further one can substitute $L_+ = b$.

As for the pair correlation function, the distribution over times, determined by the factor $\exp[-\tau S(\varrho/\tau)]$, has a peak at $\lambda\tau = \ln(b/L)$. Therefore we find after integration over times

$$F_{2n} \propto \frac{1}{b^{n+1}L_-^{n-1}}. \tag{75}$$

Since the expression (75) is determined by typical events, we can say that $L_- = LL_\star/b$ if $\lambda\tau < \ln(L_\star/r_\kappa)$ and $L_- = r_\kappa$ otherwise. Thus, we arrive at

$$F_{2n} \propto \begin{cases} b^{-2}, & L \ll b \ll LL_\star/r_\kappa, \\ b^{-n-1}, & b \gg LL_\star/r_\kappa. \end{cases} \tag{76}$$

The expressions (76) cover the pair correlation function as well. For the pair correlation function, where $n = 1$, there are no differences in the regimes of Eq. (76), in accordance with the above analysis.

It is possible to include in our consideration a linear damping of scalar of rate $\gamma$, which can be interpreted as chemical decay of concentration. For the isotropic turbulence case it was considered theoretically in [59], and in addition numerically in [60,61] via study of spatial correlations. For our flow the mathematical treatment should be similar to the one presented in the last reference. In particular, it is anticipated that the filamental-smooth transition should occur when the decay rate is equal to the Lyapunov exponent, $\gamma = \bar{\lambda}$.

## V. CONCLUSION

In the present paper we examined statistical characteristics of the passive scalar, like its moments and correlation functions, when it is mixed by shear flow with the addition of relatively weak smooth random flow in incompressible fluid. In accordance with the established criteria, we limit our consideration to the situation when the random flow is relatively weak compared to the mean flow (8) but is strong enough to produce the stirring, which is more intense than the molecular diffusion at the scale of the forcing; see (45). We considered both the problem of the passive scalar decay and the problem of its statistically homogeneous in time supply. As was expected, the statistical properties of the passive scalar appear to be far from Gaussian. Therefore, study of parameters of the passive scalar distribution cannot be reduced to the analysis of the mean square and the pair correlation function and requires examination of moments and correlation functions of higher order. We have developed the technique enabling to perform the analysis. Obtained results are expressed via the Cramér function (14) for the statistics of stretching in the given random flow and thus have rather general applicability. It turns out that after the proper rescaling in space the results have properties similar to characteristic ones from the isotropic case, being written in terms of the Cramér function for their random flow. For this reason, a statistical analysis of passive scalar advection provides information about the flow statistics itself. In our work we have established properties of the Cramér function under some general assumptions. Besides, we have provided its numerical approximation and certain analytical results in the case of a flow model with short correlated-in-time fluctuations.

The data that support the findings of this study are available from the corresponding author upon reasonable request.

## ACKNOWLEDGMENTS

The work was supported by Grant No. 20-12-00383 of RScF, and the part concerning the one-point moments was supported by the Ministry of Science and Higher Education of the Russian Federation (state assignment no. FFWR-2024-0014). The authors thank I. V. Kolokolov for valuable discussions.

## APPENDIX A: SYMMETRY OF PDF FOR THE SCALING FACTOR

In this Appendix we consider a consequence of the stochastic equations (10) and (11) for a random variable $\zeta$ with homogeneous in time statistics that is invariant under time inversion. The symmetry means that all correlation functions of $\zeta$ are invariant under the transformation $t \to -t$. Then the relation (13) is valid for the probability density function $\Pi(\varrho)$.

We consider the stochastic evolution of the variables $\varrho, \phi$ on some finite-time interval $(0, T)$ and denote as $\varrho$ the value of the variable $\varrho$ at the final moment of time, $\varrho(T)$. The function $\varrho$, as a consequence of Eq. (10), can be written via time integration,

$$\varrho = \int_0^T d\tau\,(1+\zeta)\cos\phi\sin\phi, \tag{A1}$$

where we assumed that initially $\varrho(0) = 0$. The random process $\zeta$ is supposed to possess homogeneous in time statistics.

Using Eqs. (10) and (11), one can represent $\Pi(\varrho)$ as the following path integral [62]:

$$\Pi(\varrho) = \left\langle \int \mathcal{D}\phi\,\mathcal{D}p\,\exp(iI) \times \delta\left[\varrho - \int d\tau\,(1+\zeta)\cos\phi\sin\phi\right]\right\rangle, \tag{A2}$$

$$I = \int d\tau\, p(\partial_\tau\phi + A), \tag{A3}$$

$$A(\phi) = -\zeta\cos^2\phi + \sin^2\phi, \tag{A4}$$

where $p(\tau)$ is an auxiliary field, angle field $\phi(\tau)$ with domain on a real axis, thereby containing information about rotations of $\boldsymbol{\ell}$, and angular brackets mean averaging over statistics of $\zeta$. The integration over $p$ in Eq. (A2) ensures validity of Eq. (11), and the $\delta$ function in Eq. (A2) reflects the relation (A1).

Let us apply the transformation

$$\tau \to T - \tau, \quad \phi \to -\phi, \quad \varrho \to -\varrho, \tag{A5}$$

where the last one means interchange $\varrho(0) \leftrightarrow \varrho(T)$. It is reduced to the substitution $\zeta(\tau) \to \zeta(T-\tau)$ in the effective action $I$ and in the $\delta$ function in Eq. (A2). For the statistics of $\zeta$, which is invariant under the time inversion, the averages over $\zeta(\tau)$ and $\zeta(T-\tau)$ coincide. Naively, one could conclude from Eq. (A2) that $\Pi(\varrho) = \Pi(-\varrho)$. However, caution is needed here, since the integral giving the effective action $I$ should be imposed by causality. Therefore, the time inversion is not an innocuous transformation. To clarify the point we move to time-discretized version of the integral (A3).

The integral (A3) can be written as the limit of the sum

$$I = \sum_{n=1}^{N} [p_n(\phi_n - \phi_{n-1}) + \varepsilon p_n A_{n-1}], \tag{A6}$$

$$A_n = -\zeta_n\cos^2\phi_n + \sin^2\phi_n, \tag{A7}$$

where $\varepsilon$ is the time spacing and the parameters $p_n, \phi_n$ correspond to the values of the variables $p, \phi$ at the time $\tau_n = n\varepsilon$. The value of $\phi_0$ is fixed as the initial condition. In accordance with causality, the factor at $p_n$ in Eq. (A6) corresponds to the relation $\phi_n = \phi_{n-1} + \varepsilon A_{n-1}$.

Due to the retarded structure of (A6) the normalization constant

$$\int Dp\,D\phi\,\exp(iI) \to \prod_{n=1}^{N}\int \frac{dp_n\,d\phi_n}{2\pi}\exp(iI) \tag{A8}$$

is equal to unity. To prove this property, we begin the calculation of the integral (A8) "from the end," performing first integration over the final angle, $\phi_N$, since the initial value of $\phi$, $\phi_0$, is fixed, as one should. The only term in $I$ (A6) containing $\phi_N$ is $p_N\phi_N$. Thus, the integration over $\phi_N$ produces $2\pi\delta(p_N)$ and the subsequent integration over $p_N$ is reduced to the substitution $p_N = 0$. After the integrations we return to the initial form of $I$ with the number of $p_n, \phi_n$ decreased by one. Repeating the procedure, we conclude that the normalization constant equals one.

Now we consider $\Pi(-\varrho)$, which can be found by the inversion $\tau \to T-\tau, \phi \to -\phi$ in Eq. (A2). Then we arrive at the same path integral of same form, where the effective action $I$ is substituted by $I_-$. Structure of the action $I_-$ is analogous to Eq. (A6), though shifted, with the fixed final value $\phi_{N+1}$ now

$$I_- = \sum_{m=1}^{N} [p_m(\phi_{m+1} - \phi_m) + \varepsilon p_m A_m] \to \sum_{m=1}^{N} p_m\left[\left(1 - \varepsilon\frac{\partial A_m}{\partial \phi_m}\right)(\phi_{m+1} - \phi_m) + \varepsilon A_{m+1}\right]. \quad (A9)$$

This feature leads to an additional factor at integration with the weight $\exp(iI_-)$ comparing with $\exp(iI)$ integration's weight.

To establish the factor, we consider the integral

$$\mathcal{N} = \int Dp\, D\phi\, \exp(iI_-) \to \prod_{n=1}^{N}\int \frac{dp_n\, d\phi_n}{2\pi}\exp(iI_-). \quad (A10)$$

In this case, we should start "from the beginning" since $\phi_{N+1}$ is fixed; the first integration should be performed over $\phi_1$ and gives

$$\int \frac{d\phi_1}{2\pi}\exp\left[-ip_1\left(1-\varepsilon\frac{\partial A_1}{\partial\phi_1}\right)\phi_1\right] = \frac{\delta(p_1)}{\left(1-\varepsilon\frac{\partial A_1}{\partial \phi_1}\right)}.$$

The subsequent integration over $p_1$ is reduced to substituting $p_1 = 0$.

Repeating the procedure for all $\phi_n, p_n$, one obtains

$$\mathcal{N} = \int Dp\, D\phi\, \exp(iI_-) \to \prod_{m=1}^{N}\left(1-\varepsilon\frac{\partial A_m}{\partial\phi_m}\right)^{-1} \to \exp\left(\sum_m \varepsilon\frac{\partial A_m}{\partial \phi_m}\right) \to \exp\left(\int d\tau\, \frac{\partial A}{\partial\phi}\right).$$

Due to the $\delta$ function in (A2), it is expressed via (A1) after our inversion transformation

$$2\rho(T) - 2\rho(0) = \int_0^T d\tau\,\frac{\partial A}{\partial \phi} = -2\rho, \quad (A11)$$

resulting in normalization factor:

$$\mathcal{N} = \exp(-2\varrho). \quad (A12)$$

Just the presence of this factor distinguishes the path integral with the effective action $I$ and one with the effective action $I_-$. Remembering, that the path integral with $I$ determines $\Pi(\varrho)$ and that the path integral with $I_-$ determines $\Pi(-\varrho)$, we arrive at the law (13).

As well, let us note the Fluctuation Theorem can be formulated for our dynamical system with time-invertible statistics. Following the work [41], we see that Eq. (A11) means the relative contraction of volume in phase space during evolution: $\Lambda = \partial\dot\phi/\partial\phi = -2\dot\rho$, which defines the dissipation function according to (2.6): $\overline{\Omega}_\tau = 2\xi$ for our system. The Fluctuation Theorem formula (2.8) for $\overline{\Omega}_\tau$ is our symmetry (17).

## APPENDIX B: CONNECTION TO THE UNSTRETCHED SPACE

In the works [34,63] the other ("natural") parametrization of vector $\boldsymbol{\ell}$,

$$\ell_x = l_0 \exp\rho\cos\varphi, \quad \ell_y = l_0\exp\rho\sin\varphi \quad (B1)$$

was used, which differs from our parametrization; see Sec. II A. The "natural" parametrization (B1) may be more convenient for analysis of experimental data; see, e.g., Ref. [36]. All analytical results regarding the angle dynamics and the Lyapunov exponent were obtained in Refs. [34,63] also using that parametrization. Here we demonstrate how these results can be transferred to the parametrization (9) used in our work. For brevity, we introduce below the notation $\varphi_* = (D/\Sigma)^{1/3} \ll 1$ for the characteristic value of angle $\varphi$.

Angles $\phi$ and $\varphi$ are related to each other by

$$\sin\phi = \frac{\sin\varphi}{\sqrt{(\varphi_*\cos\varphi)^2 + \sin^2\varphi}}, \quad \cos\phi = \frac{\varphi_*\cos\varphi}{\sqrt{(\varphi_*\cos\varphi)^2+\sin^2\varphi}}. \quad (B2)$$

Under the transformation (B2), points $\pi n/2$ (where $n$ is integer) remain unchanged. In particular, this means that the tumbling frequency $\omega$ (28) in terms of $\varphi$ and $\phi$ is the same. The exponents $\rho$ and $\varrho$ differ on a function whose value is bounded in time,

$$\rho = \varrho + \frac{1}{2}\ln\left(\frac{\cos^2\phi}{\varphi_*^2} + \sin^2\phi\right), \quad (B3)$$

so the Cramér function (14) and the Lyapunov exponent (27) are the same for PDF of $\rho$.

Let us derive here the approximate dynamical equations (10) and (11) in terms of $\rho$, $\varphi$. Full dynamical equations (5) and (6) written in terms of $\rho, \varphi$ are

$$\partial_t\rho = \frac{\Sigma + \partial_y u_x + \partial_x u_y}{2}\sin(2\varphi) + \partial_x u_x\cos(2\varphi), \quad (B4)$$

$$\partial_t\varphi = -(\Sigma + \partial_y u_x)\sin^2\varphi + \partial_x u_y\cos^2\varphi - \partial_x u_x \sin(2\varphi), \quad (B5)$$

where we used $\partial_y u_y = -\partial_x u_x$ due to the incompressibility. First, we neglect all terms where $\partial_i u_j$ is added to $\Sigma$ as we assume that the steady effect produced by $\Sigma$ is stronger than one produced by the flow fluctuations $\partial_i u_j$ at the relevant timescale $1/\lambda$. Due to the correlation time of $\partial_i u_j$ being smaller than this timescale, we obtain the requirement $\Sigma/\lambda \gg \sqrt{D/\lambda}$ for each element of tensor $D$ in (7), which is ensured with our basic assumption (8): $\Sigma \gg D$. Next, due to the estimation for angle $|\sin\varphi| \sim \varphi_*$, we neglect the last terms in (B4) and (B5) as their effect is relatively small as $\sqrt{D/\lambda} \sim \varphi_* \ll 1$. Thus we arrive at

$$\partial_t\rho = \frac{\Sigma}{2}\sin(2\varphi), \quad \partial_t\varphi = -\Sigma\sin^2\varphi + \partial_x u_y\cos(2\varphi), \quad (B6)$$

which corresponds to (10) and (11) written in terms of $\rho, \varphi$. Note that within the used accuracy one can replace $\cos(2\varphi)$ by unity in (B6), since the term is relevant only when $|\sin\varphi| \lesssim \varphi_*$. This derivation is equivalent in respect of neglected terms in (B5) to the ones in [33,34]. Within the Langevin model

(26), noise in Eq. (B6) has the statistics determined by the pair correlation function $\langle \partial_x u_y(t)\partial_x u_y(t')\rangle = 2D\delta(t-t')$. Comparing the order of terms in system (B6) at angle values $|\sin\varphi| \sim \varphi_*$ where fluctuations are relevant, one obtains the characteristic timescale (which is an order of tumbling frequency as well) via estimate for Lyapunov exponent: $t_*^{-1} = \bar\lambda \sim \Sigma\varphi_* \sim \Sigma\sqrt{D/\bar\lambda}$, that gives $\bar\lambda \sim D^{1/3}\Sigma^{2/3}$.

Equations (B6) were obtained and treated analytically in [34,63] in the limit of small parameter $D/\Sigma \ll 1$. In particular, analytical expressions for $\lambda$ and $\omega$ (31) can be found there. Also, there is the stationary solution for PDF $Q_s(\varphi)$, which is an analog of $P_s(\phi)$, with a narrow peak at $\varphi \sim \varphi_*$ of the same width $\sim\varphi_*$ and the algebraic tails $Q_s = \omega\varphi_*/\pi \sin^2\varphi$.

## APPENDIX C: CONNECTION BETWEEN THE STATISTICS OF LAGRANGIAN TRAJECTORIES AND THE PAIR CORRELATION FUNCTION

In this Appendix we derive Eq. (35) for $\mathcal{F}(t,\boldsymbol{r})$ and establish the equation for the pair correlation function $F(t,\boldsymbol{r})$ in case of the short correlated model determined by Eq. (26). The function $F$ can be related to the joint PDF $\mathcal{P}(\phi,\varrho)$.

The dynamics of object $\mathcal{F}(t,\boldsymbol{r}_1,\boldsymbol{r}_2) = \langle\vartheta(t,\boldsymbol{r}_1)\vartheta(t,\boldsymbol{r}_2)\rangle_\vartheta$, where low index $\vartheta$ means over the statistics of the forcing $f$ or the initial conditions, follows from the basic equation (1):

$$\partial_t\mathcal{F} = -[(\boldsymbol{v}^{(1)}\nabla^{(1)}) + (\boldsymbol{v}^{(2)}\nabla^{(2)})]\mathcal{F} + (\Delta^{(1)} + \Delta^{(2)})\mathcal{F} + \langle\vartheta^{(1)}f^{(2)} + \vartheta^{(2)}f^{(1)}\rangle_\vartheta. \tag{C1}$$

Here indices (1) and (2) mean points $\boldsymbol{r}_1$ and $\boldsymbol{r}_2$ respectively. If the statistics of the scalar is homogeneous in space, then $\mathcal{F}$ depends on $\boldsymbol{r} = \boldsymbol{r}_2 - \boldsymbol{r}_1$ only. Then the sum of Laplacians is $\Delta^{(1)} + \Delta^{(2)} = 2\Delta$, and the advection term is $(\boldsymbol{v}^{(1)}\nabla^{(1)}) + (\boldsymbol{v}^{(2)}\nabla^{(2)}) = (\boldsymbol{v}^{(2)} - \boldsymbol{v}^{(1)})\nabla$, where differentiation with respect to components of $\boldsymbol{r}$. Next, employing the smoothness of velocity field (4), we simplify the advection term to $(\partial_i v_j)r_i\partial_j$, which we divide then in (35) into the constant and random parts. The last term in (C1) is relevant only if there is stochastic forcing and equals to $\Theta$ (66).

Now let us derive equation for $F$, first within the decay problem. Equation (36) averaged over statistics of the random flow (26) takes the form

$$\partial_\tau F + y\partial_w F - w^2\partial_y^2 F = r_\kappa^2\partial_y^2 F. \tag{C2}$$

One can neglect the diffusion at scales much larger than $r_\kappa$. The absence of diffusion means that the pair correlation function is determined only by the statistics of Lagrangian trajectories. In other words, Eq. (C2) should be equivalent to Eq. (32). To prove the property, we introduce

$$F = \mathcal{P}/b^2, \tag{C3}$$

where $b$ and $\psi$ are defined in (56). Then Eq. (C2) written in terms of $\mathcal{P}$, $\varrho = \ln b$, and $\phi = \psi$ coincides with Eq. (32).

Next we turn to the problem of continuous forcing. The pair correlation function satisfies the same equation (C2) with additional term $\Theta(\boldsymbol{r})$, which is the spacial correlation function of the forcing, describing the supply [see Eq. (66)]:

$$\partial_\tau F + y\partial_w F - w^2\partial_y^2 F = r_\kappa^2\partial_y^2 F + \Theta. \tag{C4}$$

To consider the Batchelor (downscale) cascade of the passive scalar, it is instructive to rewrite Eq. (C4) in Fourier space,

$$\left(\partial_\tau - k_w\partial_{k_y} - k_y^2\partial_{k_w}^2 + r_\kappa^2 k_y^2\right)\widetilde{F}_{\mathbf{k}} = \widetilde{\Theta}_{\mathbf{k}}, \tag{C5}$$

where the Fourier transform is determined in accordance with

$$\widetilde{F}_{\mathbf{k}}(t) = \int \mathrm{d}w\,\mathrm{d}y\,F(t,\boldsymbol{r})\exp(-ik_w w - ik_y y). \tag{C6}$$

We consider (C5) in the inertial range $1/L_\star \ll k = \sqrt{k_w^2 + k_y^2} \ll 1/r_\kappa$, where diffusion and supply terms are negligible. In case of the shear flow, there is a symmetry with the equation in coordinate space: in the absence of diffusion, Eq. (C5) is equivalent to Eq. (C4) under change $\{k_w, k_y\} \to \{y, -w\}$. Therefore, there is the stationary solution of (C5) in the inertial range, which corresponds to the Batchelor cascade

$$\widetilde{F}_{\mathbf{k}} = \frac{2\pi^2\Theta(0)\,P_s(\phi_k)}{\bar\lambda k^2}, \tag{C7}$$

where $k_y = k\cos\phi_k$, $k_w = -k\sin\phi_k$, and $P_s$ is the stationary angle PDF (32). The factor with forcing $\Theta$ here comes from the requirement that the flux through line $k = \text{const}$ should be equal to the scalar variance production rate $\Theta(0)$. The spectrum is obtained from (C7) via integration over angle is $k/(2\pi)^2\int \mathrm{d}\psi\,\widetilde{F}_{\mathbf{k}} = \Theta(0)/(\bar\lambda k)$. The $k^{-1}$ dependence is the same as for isotropic turbulence case [8] and corresponds to logarithmic dependence (73) in $b$ space. The inverse Fourier transform of (C7) brings us to (73).

## APPENDIX D: FOURIER TRANSFORM

Here we analyze properties of Fourier transform of the joint PDF $\mathcal{P}(\tau,\varrho,\phi)$ determined by Eq. (33). One can write Eq. (32) in the form

$$\partial_\tau\widetilde{\mathcal{P}} = -\hat{M}\widetilde{\mathcal{P}}, \tag{D1}$$

$$\hat{M} = (\eta-1)\cos\phi\sin\phi - \sin\phi\,\partial_\phi\sin\phi - [\cos\phi\sin\phi\,(\eta-1) + \cos\phi\,\partial_\phi\cos\phi]^2. \tag{D2}$$

Thus, we arrive at the differential equation formulated solely in terms of the angle $\phi$.

A general solution of Eq. (D1) can be written as

$$\widetilde{\mathcal{P}}(\tau,\phi,\eta) = \sum_n c_n\exp[-\gamma_n(\eta)\tau]\widetilde{\mathcal{P}}_n(\phi,\eta), \tag{D3}$$

where factors $c_n$ depend on initial conditions. Here $\widetilde{\mathcal{P}}_n$ are eigenfunctions of the operator $\hat{M}(\eta)$ with the corresponding eigenvalue $\gamma_n(\eta)$:

$$\hat{M}\widetilde{\mathcal{P}}_n = \gamma_n\widetilde{\mathcal{P}}_n.$$

The discreteness of the eigenfunctions $\widetilde{\mathcal{P}}_n$ is caused by their periodicity in $\phi$.

If $\gamma_n$ is the eigenvalue of the operator $\hat{M}$ for a given value of $\eta$, there is the same eigenvalue $\gamma_n$ for $2-\eta$. To prove the assertion we consider the matrix

$$M_{mn} = \int_{-\pi/2}^{\pi/2}\frac{d\phi}{\pi}\exp(-2im\phi)\hat{M}\exp(2in\phi), \tag{D4}$$

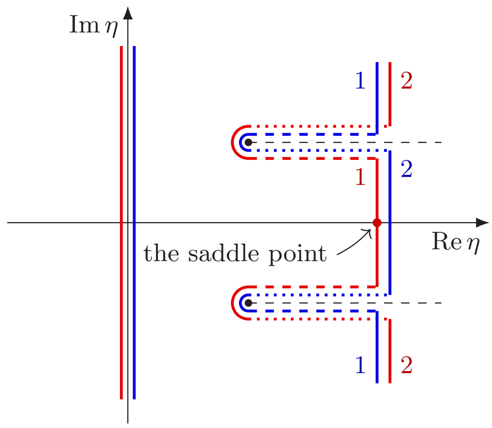


FIG. 2. Integration contours for the inverse Fourier transform. Continuous blue and red straight lines along the imaginary axis are the initial contours of the integration. Dashed black lines are branch cuts.

which eigenvalues are $\gamma_n(\eta)$ by definition. Let us consider the transposed matrix $M_{nm}$. Substituting $\phi \to -\phi$ in integral (D4) for $M_{nm}$ and integrating over $\phi$ by parts, we find $M_{nm}(\eta) = M_{mn}(2-\eta)$. Since the eigenvalues of a matrix and of a transposed one are the same, we find that eigenvalue sets of the operators $\hat{M}(\eta)$ and $\hat{M}(2-\eta)$ coincide, which concludes the assertion's proof.

At large times, the main contribution to the sum (D3) at a given $\eta$ is produced by the term with $\gamma_n$, whose real part is the smallest (we denote it as $\gamma$). In fact, eigenvalues $\gamma_n$ are ordered by increase of Re $\gamma_n$. Since

$$\widetilde{\Pi} = \int_{-\pi/2}^{+\pi/2} \frac{d\phi}{\pi} \widetilde{\mathcal{P}}(\tau, \phi, \eta),$$

we conclude that just one term with this $\gamma$ enters Eq. (21). This fact enables one to find $\gamma(\eta)$ numerically, by solving the equation $\hat{M}\widetilde{\mathcal{P}}_n = \gamma_n \widetilde{\mathcal{P}}_n$.

There are singular points in $\eta$ complex plane, where a pair of eigenvalue branches, $\gamma_i(\eta)$ and $\gamma_j(\eta)$ approach the same value. In particular, the zeroth eigenvalue coincides with the next first eigenvalue at points $\eta - 1 \approx \pm 2.1 \pm 1.6i$, and the next two, first and second, eigenvalues with the smallest real parts are equal to each other in the points $\eta - 1 \approx \pm 5.0$. In the vicinity of such a point, each of the corresponding eigenvalues acts as one of two branches of a square-root-like singularity. It is important that the singularities produce zero contributions to the inverse Fourier transform

$$\mathcal{P} = \int \frac{d\eta}{2\pi i} \exp(\varrho\eta)\widetilde{\mathcal{P}}, \tag{D5}$$

at large $|\varrho|$. Let us take negative $\varrho$; then one should deform two contours of the integral which correspond to the involved eigenvalues as depicted in Fig. 2. The integrands including pre-exponents, considered as analytical continuation from the real axis, are equal to each other on the dotted parts of the deformed contours, but the directions of the contours are opposite, so the results of integrations along the contours' dotted parts cancel each other. The same holds for the dashed parts of the contours. Because of branch points' square-root-like behavior, one can reassemble the integration contours after passing the point into a new pair of contours from the pieces, which are marked as "1" and "2" in Fig. 2. Therefore, we conclude that moving integration contours in the pairs on the complex plane allow one to not consider such singular branch points.

In that way, at large times the inverse Fourier transform is determined by the zeroth eigenvalue and eigenfunction and the corresponding saddle point located on the real axis, which ensures the positiveness of the PDF $\mathcal{P}$. The saddle point satisfies Eq. (23): $\eta = -\partial_\xi S(\xi)$. Knowing $\gamma(\eta)$, one finds the Cramér function via the Legendre transform. The result is consistent with the statistics obtained via numerical simulation of Langevin equations (10) and (11). Note that the Cramér function $S(\xi) \approx 0.33\xi^4$ at large $|\xi| \gg 1$. This extremely fast decay of the PDF stops at $|\xi| \sim (\Sigma/D)^{2/3}$, and after that the Cramér function $S \sim (\varrho/Dt)^2$, that is provided by terms with the derivatives of $\boldsymbol{u}$ in Eqs. (5) and (6), omitted in our analysis.

[1] G. Falkovich, K. Gawędzki, and M. Vergassola, Particles and fields in fluid turbulence, Rev. Mod. Phys. **73**, 913 (2001).
[2] E. Villermaux, Mixing versus stirring, Annu. Rev. Fluid Mech. **51**, 245 (2019).
[3] A. N. Kolmogorov, Equations of turbulent motion in an incompressible fluid, Dokl. Akad. Nauk SSSR **30**, 299 (1941).
[4] R. H. Kraichnan, Inertial ranges in two-dimensional turbulence, Phys. Fluids **10**, 1417 (1967).
[5] A. M. Obukhov, Structure of the temperature field in a turbulent flow, Izvestiya Akad. Nauk SSSR, Seriya Geograficheskaya i Geofizicheskaya **13**, 58 (1949).
[6] S. Corrsin, On the spectrum of isotropic temperature fluctuations in an isotropic turbulence, J. Appl. Phys. **22**, 469 (1951).
[7] G. K. Batchelor, Small-scale variation of convected quantities like temperature in turbulent fluid part 1. General discussion and the case of small conductivity, J. Fluid Mech. **5**, 113 (1959).
[8] D. A. Donzis, K. Sreenivasan, and P. Yeung, The Batchelor spectrum for mixing of passive scalars in isotropic turbulence, Flow, Turbul. Combust. **85**, 549 (2010).
[9] K. R. Sreenivasan, Turbulent mixing: A perspective, Proc. Natl. Acad. Sci. USA **116**, 18175 (2019).
[10] L. Prandtl, *Aerodynamic Theory* (Springer, Berlin Julius, 1935), Vol. III, pp. 34–208.
[11] J. Jiménez, Near-wall turbulence, Phys. Fluids **25**, 101302 (2013).
[12] A. J. Smits, B. J. McKeon, and I. Marusic, High–Reynolds number wall turbulence, Annu. Rev. Fluid Mech. **43**, 353 (2011).
[13] E. Germaine, L. Mydlarski, and L. Cortelezzi, Persistence of local anisotropy of passive scalars in wall-bounded flows, Phys. Rev. Fluids **3**, 014606 (2018).
[14] H. Xia, M. Shats, and G. Falkovich, Spectrally condensed turbulence in thin layers, Phys. Fluids **21**, 125101 (2009).

[15] J. Laurie, G. Boffetta, G. Falkovich, I. Kolokolov, and V. Lebedev, Universal profile of the vortex condensate in two-dimensional turbulence, Phys. Rev. Lett. **113**, 254503 (2014).
[16] I. V. Kolokolov and V. V. Lebedev, Structure of coherent vortices generated by the inverse cascade of two-dimensional turbulence in a finite box, Phys. Rev. E **93**, 033104 (2016).
[17] I. Kolokolov and V. Lebedev, Velocity statistics inside coherent vortices generated by the inverse cascade of 2-D turbulence, J. Fluid Mech. **809**, R2 (2016).
[18] A. Groisman and V. Steinberg, Efficient mixing at low Reynolds numbers using polymer additives, Nature **410**, 905 (2001).
[19] M. Chertkov, C. Connaughton, I. Kolokolov, and V. Lebedev, Dynamics of energy condensation in two-dimensional turbulence, Phys. Rev. Lett. **99**, 084501 (2007).
[20] A. Groisman and V. Steinberg, Elastic turbulence in a polymer solution flow, Nature (London) **405**, 53 (2000).
[21] V. Steinberg, Elastic turbulence: An experimental view on inertialess random flow, Annu. Rev. Fluid Mech. **53**, 27 (2021).
[22] M. Speetjens, G. Metcalfe, and M. Rudman, Lagrangian transport and chaotic advection in three-dimensional laminar flows, Appl. Mech. Rev. **73**, 030801 (2021).
[23] Z. Liu, M. F. Speetjens, A. J. Frijns, and A. A. van Steenhoven, Application of astigmatism $\mu$-PTV to analyze the vortex structure of AC electroosmotic flows, Microfluid. Nanofluid. **16**, 553 (2014).
[24] H. Feng, M. G. Olsen, Y. Liu, R. O. Fox, and J. C. Hill, Investigation of turbulent mixing in a confined planar-jet reactor, AIChE J. **51**, 2649 (2005).
[25] T. Burghelea, E. Segre, I. Bar-Joseph, A. Groisman, and V. Steinberg, Chaotic flow and efficient mixing in a microchannel with a polymer solution, Phys. Rev. E **69**, 066305 (2004).
[26] Y. Amarouchene and H. Kellay, Batchelor scaling in fast-flowing soap films, Phys. Rev. Lett. **93**, 214504 (2004).
[27] Y. Jun and V. Steinberg, Mixing of passive tracers in the decay Batchelor regime of a channel flow, Phys. Fluids **22**, 123101 (2010).
[28] D. Son, Turbulent decay of a passive scalar in the Batchelor limit: Exact results from a quantum-mechanical approach, Phys. Rev. E **59**, R3811 (1999).
[29] E. Balkovsky and A. Fouxon, Universal long-time properties of Lagrangian statistics in the Batchelor regime and their application to the passive scalar problem, Phys. Rev. E **60**, 4164 (1999).
[30] S. Vergeles, Spatial dependence of correlation functions in the decay problem for a passive scalar in a large-scale velocity field, J. Exp. Theor. Phys. **102**, 685 (2006).
[31] M. Souzy, I. Zaier, H. Lhuissier, T. Le Borgne, and B. Metzger, Mixing lamellae in a shear flow, J. Fluid Mech. **838**, R3 (2018).
[32] A. Celani, M. Cencini, M. Vergassola, E. Villermaux, and D. Vincenzi, Shear effects on passive scalar spectra, J. Fluid Mech. **523**, 99 (2005).
[33] M. Chertkov, I. Kolokolov, V. Lebedev, and K. Turitsyn, Polymer statistics in a random flow with mean shear, J. Fluid Mech. **531**, 251 (2005).
[34] K. Turitsyn, Polymer dynamics in chaotic flows with a strong shear component, J. Exp. Theor. Phys. **105**, 655 (2007).
[35] D. E. Smith, H. P. Babcock, and S. Chu, Single-polymer dynamics in steady shear flow, Science **283**, 1724 (1999).
[36] Y. Liu and V. Steinberg, Stretching of polymer in a random flow: Effect of a shear rate, Europhys. Lett. **90**, 44005 (2010).
[37] M. Šiler, L. Ornigotti, O. Brzobohatý, P. Jákl, A. Ryabov, V. Holubec, P. Zemánek, and R. Filip, Diffusing up the hill: Dynamics and equipartition in highly unstable systems, Phys. Rev. Lett. **121**, 230601 (2018).
[38] N. Ivchenko and S. Vergeles, Statistics of a passive scalar in a 2D shear flow with fluctuations, J. Exp. Theor. Phys. **136**, 644 (2023).
[39] B. I. Shraiman and E. D. Siggia, Lagrangian path integrals and fluctuations in random flow, Phys. Rev. E **49**, 2912 (1994).
[40] D. J. Searles and D. J. Evans, Fluctuation theorem for stochastic systems, Phys. Rev. E **60**, 159 (1999).
[41] D. J. Evans and D. J. Searles, The fluctuation theorem, Adv. Phys. **51**, 1529 (2002).
[42] W. Feller, *An Introduction to Probability Theory and Its Applications* (Wiley, New York, 1971), Vol. II.
[43] A. Klenke, *Probability Theory: A Comprehensive Course* (Springer-Verlag London, 2007).
[44] P. H. Haynes and J. Vanneste, What controls the decay of passive scalars in smooth flows? Phys. Fluids **17**, 097103 (2005).
[45] B. K. Øksendal, *Stochastic Differential Equations: An Introduction with Applications*, 6th ed. (Springer-Verlag Berlin Heidelberg, 2003).
[46] F. C. Klebaner, *Introduction to Stochastic Calculus with Applications*, 2nd ed. (Imperial College Press, London, 2005).
[47] G. Wick, The evaluation of the collision matrix, Phys. Rev. **80**, 268 (1950).
[48] S. Corrsin, The decay of isotropic temperature fluctuations in an isotropic turbulence, J. Aeronaut. Sci. **18**, 417 (1951).
[49] M. Avellaneda and A. J. Majda, Superdiffusion in nearly stratified flows, J. Stat. Phys. **69**, 689 (1992).
[50] J. Vanneste, Intermittency of passive-scalar decay: Strange eigenmodes in random shear flows Phys. Fluids **18**, 087108 (2006).
[51] A. J. Majda, The random uniform shear layer: An explicit example of turbulent diffusion with broad tail probability distributions, Phys. Fluids **5**, 1963 (1993).
[52] J. Duplat, C. Innocenti, and E. Villermaux, A nonsequential turbulent mixing process, Phys. Fluids **22**, 035104 (2010).
[53] D. R. Fereday and P. H. Haynes, Scalar decay in two-dimensional chaotic advection and Batchelor-regime turbulence, Phys. Fluids **16**, 4359 (2004).
[54] T. M. Antonsen Jr., Z. Fan, E. Ott, and E. Garcia-Lopez, The role of chaotic orbits in the determination of power spectra of passive scalars, Phys. Fluids **8**, 3094 (1996).
[55] J. Sukhatme and R. T. Pierrehumbert, Decay of passive scalars under the action of single scale smooth velocity fields in bounded two-dimensional domains: From non-self-similar probability distribution functions to self-similar eigenmodes, Phys. Rev. E **66**, 056302 (2002).
[56] J.-L. Thiffeault, Scalar decay in chaotic mixing, *Transport and Mixing in Geophysical Flows* (Springer-Verlag, Berlin, Heidelberg, 2008), pp. 3–36.

[57] V. L. M. Chertkov and I. Kolokolov, Strong effect of weak diffusion on scalar turbulence at large scales, Phys. Fluids **19**, 101703 (2007).

[58] I. Kolokolov and N. T. Trung, Statistical properties of passive scalar in a random flow with a strong shear component, Phys. Lett. A **376**, 1836 (2012).

[59] M. Chertkov, On how a joint interaction of two innocent partners (smooth advection and linear damping) produces a strong intermittency, Phys. Fluids **10**, 3017 (1998).

[60] Z. Neufeld, C. López, E. Hernández-García, and T. Tél, Multifractal structure of chaotically advected chemical fields, Phys. Rev. E **61**, 3857 (2000).

[61] A. Tzella and P. H. Haynes, Smooth and filamental structures in chaotically advected chemical fields, Phys. Rev. E **81**, 016322 (2010).

[62] R. P. Feynman and A. R. Hibbs, *Quantum Mechanics and Path Integrals* (McGraw-Hill, New York, 1965).

[63] A. Puliafito and K. Turitsyn, Numerical study of polymer tumbling in linear shear flows, Physica D **211**, 9 (2005).